defines a new subfamily of differentially expressed neural cell adhesion molecules. *J. Neurosci. 15*, 2141–2156.
14. Brauer, A. U., Savaskan, N. E., Plaschke, M., Prehn, S., Ninnemann, O., and Nitsch, R. (2000) IG-molecule Kilon shows differential expression pattern from LAMP in the developing and adult rat hippocampus. *Hippocampus 10*, 632–644.
15. Gil, O. D., Zhang, L., Chen, S., Ren, Y. Q., Pimenta, A., Zanazzi, G., Hillman, D., Levitt, P., and Salzer, J. L. (2002) Complementary expression and heterophilic interactions between IgLON family members neurotrimin and LAMP. *J. Neurobiol. 51*, 190–204.
16. Hachisuka, A., Nakajima, O., Yamazaki, T., and Sawada, J. (2000) Developmental expression of opioid-binding cell adhesion molecule (OBCAM) in rat brain. *Brain Res. Dev. Brain Res. 122*, 183–191.
17. Miyata, S., Matsumoto, N., Taguchi, K., Akagi, A., Iino, T., Funatsu, N., and Maekawa, S. (2003) Biochemical and ultrastructural analyses of IgLON cell adhesion molecules, Kilon and OBCAM in the rat brain. *Neuroscience 117*, 645–658.
18. Zacco, A., Cooper, V., Chantler, P. D., Fisher-Hyland, S., Horton, H. L., and Levitt, P. (1990) Isolation, biochemical characterization and ultrastructural analysis of the limbic system-associated membrane protein (LAMP), a protein expressed by neurons comprising functional neural circuits. *J. Neurosci. 10*, 73–90.
19. Hachisuka, A., Yamazaki, T., Sawada, J., and Terao, T. (1996) Characterization and tissue distribution of opioid-binding cell adhesion molecule (OBCAM) using monoclonal antibodies. *Neurochem. Int. 28*, 373–379.
20. Wada, Y., Tajiri, M., and Yoshida, S. (2004) Hydrophilic affinity isolation and MALDI multiple-stage tandem mass spectrometry of glycopeptides for glycoproteomics. *Anal. Chem. 76*, 6560–6565.
21. Wuhrer, M., Hokke, C. H., and Deelder, A. M. (2004) Glycopeptide analysis by matrix-assisted laser desorption/ionization tandem time-of-flight mass spectrometry reveals novel features of horseradish peroxidase glycosylation. *Rapid Commun. Mass Spectrom. 18*, 1741–1748.
22. Satomi, Y., Shimonishi, Y., and Takao, T. (2004) N-Glycosylation at Asn(491) in the Asn-Xaa-Cys motif of human transferrin. *FEBS Lett. 576*, 51–56.
23. Zaia, J. (2004) Mass spectrometry of oligosaccharides. *Mass Spectrom. Rev. 23*, 161–227.
24. Wuhrer, M., Catalina, M. I., Deelder, A. M., and Hokke, C. H. (2007) Glycoproteomics based on tandem mass spectrometry of glycopeptides. *J. Chromatogr., B: Anal. Technol. Biomed. Life Sci 849*, 115–128.
25. Wuhrer, M., Koeleman, C. A., Hokke, C. H., and Deelder, A. M. (2005) Protein glycosylation analyzed by normal-phase nano-liquid chromatography-mass spectrometry of glycopeptides. *Anal. Chem. 77*, 886–894.
26. Harazono, A., Kawasaki, N., Kawanishi, T., and Hayakawa, T. (2005) Site-specific glycosylation analysis of human apolipoprotein B100 using LC/ESI MS/MS. *Glycobiology 15*, 447–462.
27. Sandra, K., Devreese, B., Van Beeumen, J., Stals, I., and Claeyssens, M. (2004) The Q-Trap mass spectrometer, a novel tool in the study of protein glycosylation. *J. Am. Soc. Mass Spectrom. 15*, 413–423.
28. Itoh, S., Kawasaki, N., Harazono, A., Hashii, N., Matsuishi, Y., Kawanishi, T., and Hayakawa, T. (2005) Characterization of a gel-separated unknown glycoprotein by liquid chromatography/multistage tandem mass spectrometry: Analysis of rat brain Thy-1 separated by sodium dodecyl sulfate-polyacrylamide gel electrophoresis. *J. Chromatogr., A 1094*, 105–117.
29. Bordier, C. (1981) Phase separation of integral membrane proteins in Triton X-114 solution. *J. Biol. Chem. 256*, 1604–1607.
30. Lisanti, M. P., Sargiacomo, M., Graeve, L., Saltiel, A. R., and Rodriguez-Boulan, E. (1988) Polarized apical distribution of glycosyl-phosphatidylinositol-anchored proteins in a renal epithelial cell line. *Proc. Natl. Acad. Sci. U.S.A. 85*, 9557–9561.
31. Itoh, S., Kawasaki, N., Ohta, M., and Hayakawa, T. (2002) Structural analysis of a glycoprotein by liquid chromatography-mass spectrometry and liquid chromatography with tandem mass spectrometry. Application to recombinant human thrombomodulin. *J. Chromatogr., A 978*, 141–152.
32. Kikuchi, M., Hatano, N., Yokota, S., Shimozawa, N., Imanaka, T., and Taniguchi, H. (2004) Proteomic analysis of rat liver peroxisome: Presence of peroxisome-specific isozyme of Lon protease. *J. Biol. Chem. 279*, 421–428.
33. Nakajima, O., Hachisuka, A., Takagi, K., Yamazaki, T., Ikebuchi, H., and Sawada, J. (1997) Expression of opioid-binding cell adhesion molecule (OBCAM) and neurotrimin (NTM) in *E. coli* and their reactivity with monoclonal anti-OBCAM antibody. *NeuroReport 8*, 3005–3008.
34. Horstkorte, R., Schachner, M., Magyar, J. P., Vorherr, T., and Schmitz, B. (1993) The fourth immunoglobulin-like domain of NCAM contains a carbohydrate recognition domain for oligomannosidic glycans implicated in association with L1 and neurite outgrowth. *J. Cell Biol. 121*, 1409–1421.
35. Chen, Y. J., Wing, D. R., Guile, G. R., Dwek, R. A., Harvey, D. J., and Zamze, S. (1998) Neutral N-glycans in adult rat brain tissue: Complete characterisation reveals fucosylated hybrid and complex structures. *Eur. J. Biochem. 251*, 691–703.
36. Nakakita, S., Natsuka, S., Ikenaka, K., and Hase, S. (1998) Development-dependent expression of complex-type sugar chains specific to mouse brain. *J. Biochem. 123*, 1164–1168.
37. Kitamura, N., Ikekita, M., Sato, T., Akimoto, Y., Hatanaka, Y., Kawakami, H., Inomata, M., and Furukawa, K. (2005) Mouse Na^+/K^+-ATPase β1-subunit has a K^+-dependent cell adhesion activity for β-GlcNAc-terminating glycans. *Proc. Natl. Acad. Sci. U.S.A. 102*, 2796–2801.

BI8009778

Immunology
The journal of cells, molecules, systems and technologies
British Society for immunology

IMMUNOLOGY ORIGINAL ARTICLE

Alteration of *N*-glycosylation in the kidney in a mouse model of systemic lupus erythematosus: relative quantification of *N*-glycans using an isotope-tagging method

Noritaka Hashii,[1,2] Nana Kawasaki,[1,2] Satsuki Itoh,[1] Yukari Nakajima,[1,2] Toru Kawanishi[1] and Teruhide Yamaguchi[1]

[1]*Division of Biological Chemistry and Biologicals, National Institute of Health Sciences, Setagaya-ku, Tokyo, Japan, and* [2]*Core Research for Evolutional Science and Technology (CREST) of the Japan Science and Technology Agency (JST), Kawaguchi City, Saitama, Japan*

doi:10.1111/j.1365-2567.2008.02898.x
Received 19 March 2008; revised 28 May 2008; accepted 2 June 2008.
Correspondence: N. Kawasaki, Division of Biological Chemistry and Biologicals, National Institute of Health Sciences, 1-18-1 Kamiyouga, Setagaya-ku, Tokyo 158-8501, Japan. Email: nana@nihs.go.jp
Senior author: Teruhide Yamaguchi, email: yamaguch@nihs.go.jp

Summary

Changes in the glycan structures of some glycoproteins have been observed in autoimmune diseases such as systemic lupus erythematosus (SLE) and rheumatoid arthritis. A deficiency of α-mannosidase II, which is associated with branching in *N*-glycans, has been found to induce SLE-like glomerular nephritis in a mouse model. These findings suggest that the alteration of the glycosylation has some link with the development of SLE. An analysis of glycan alteration in the disordered tissues in SLE may lead to the development of improved diagnostic methods and may help to clarify the carbohydrate-related pathogenic mechanism of inflammation in SLE. In this study, a comprehensive and differential analysis of *N*-glycans in kidneys from SLE-model mice and control mice was performed by using the quantitative glycan profiling method that we have developed previously. In this method, a mixture of deuterium-labelled *N*-glycans from the kidneys of SLE-model mice and non-labelled *N*-glycans from kidneys of control mice was analysed by liquid chromatography/mass spectrometry. It was revealed that the low-molecular-mass glycans with simple structures, including agalactobiantennary and paucimannose-type oligosaccharides, markedly increased in the SLE-model mouse. On the other hand, fucosylated and galactosylated complex type glycans with high branching were decreased in the SLE-model mouse. These results suggest that the changes occurring in the *N*-glycan synthesis pathway may cause the aberrant glycosylations on not only specific glycoproteins but also on most of the glycoproteins in the SLE-model mouse. The changes in glycosylation might be involved in autoimmune pathogenesis in the model mouse kidney.

Keywords: isotope-tagging method; liquid chromatography/multiple-stage mass spectrometry; systemic lupus erythematosus

Introduction

Glycosylation is one of the most common post-translational modifications[1,2] and contributes to many biological processes, including protein folding, secretion, embryonic development and cell–cell interactions.[3] Alteration of glycosylation is associated with several diseases, including inflammatory responses and malignancies;[4–6] for instance, significant increases in fucosylation and branching are found in ovarian cancer and lung cancer.[7] Additionally, the carbohydrate structure changes from type I glycans (Galβ1-3GlaNAc) to type II glycans (Galβ1-4GalNAc) in carcinoembryonic antigen in colon cancer.[8] Furthermore, an increase in biantennary oligosaccharides lacking galactose (Gal) was found on immunoglobulin G (IgG) in systemic lupus erythematosus (SLE) and rheumatoid arthritis,[9–11] and agalactoglycans are used for the early diagnosis of rheumatoid arthritis.[12]

Systemic lupus erythematosus is an autoimmune disease characterized as chronic and as a systemic disease, with symptoms such as kidney failure, arthritis and erythema. In addition to the known changes in glycosylation on IgG, there have been several reports on the association between glycosylation and inflammation in SLE and rheumatoid

arthritis.[13–15] A deficiency of α-mannosidase II (αM-II), which is associated with branching in *N*-glycans, has been found to induce human SLE-like glomerular nephritis in a mouse model.[16] Green *et al.* reported that branching structures of *N*-glycan in mammals are involved in protection against immune responses in autoimmune disease pathogenesis.[17] Although there is no direct evidence that alteration of glycosylation is the upstream event in the pathogenesis of SLE, these findings suggest that changes in the glycan structure may be involved in the inflammatory-related autoimmune disorder. Glycosylation analysis may lead to the development of improved diagnostic methods and may help to clarify the carbohydrate-related pathogenic mechanism of inflammation in SLE.

Mass spectrometry (MS) and liquid chromatography/mass spectrometry (LC/MS) are the most prevalent strategies for identifying disease-related glycans in glycomics.[18–20] Aberrant glycosylations in some disease samples have been found by comparing mass spectra or chromatograms between normal and disease samples; however, because of the tremendous heterogeneities of the sugar moiety in glycoprotein as well as the low reproducibility of LC/MS, accurate quantitative analysis is difficult using MS and LC/MS alone. To overcome these problems, we previously developed the stable isotope-tagging method for the quantitative profiling of glycans using 2-aminopyridine (AP).[21] After the glycans are released from sample and the reference glycoproteins are derivatized to pyridyl amino (d_0-PA) glycans and to tetra-deuterium-labelled pyridyl amino (d_4-PA) glycans, respectively, a mixture of both d_0-PA and d_4-PA glycans was subjected to LC/MS, and the levels of individual glycans were calculated from the intensity ratios of d_0-glycan and d_4-glycan molecular ions (Fig. 1a). Recently, alternative isotope-tagging methods using deuterium-labelled compounds, such as 2-aminobenzoic acid its derivatives, and permethylation, have been proposed by other groups.[22–24] All of these studies prove the utility of isotope-tagging methods for the quantitative analysis of glycosylation.

In the present study, we used the isotope-tagging method to analyse changes in *N*-glycosylation in the disordered kidney in an SLE mouse model. We used an MRL/MpJ-lpr/lpr (MRL-lpr) mouse which lacks the Fas antigen gene.[25–27] The MRL-lpr mouse is known to naturally develop SLE-like glomerular nephritis and is widely used in SLE studies. MRL/MpJ-+/+ (MRL-+/+) mice were used as controls.

Materials and methods

Materials

The kidneys of the SLE-model mice (MRL-lpr) and control mice (MRL-+/+) ($n = 3$) were purchased from Japan SLC, Inc. (Hamamatsu, Japan). Thermolysin (EC 3.4.24.27), originating from *Bacillus thermoproteolyticus*

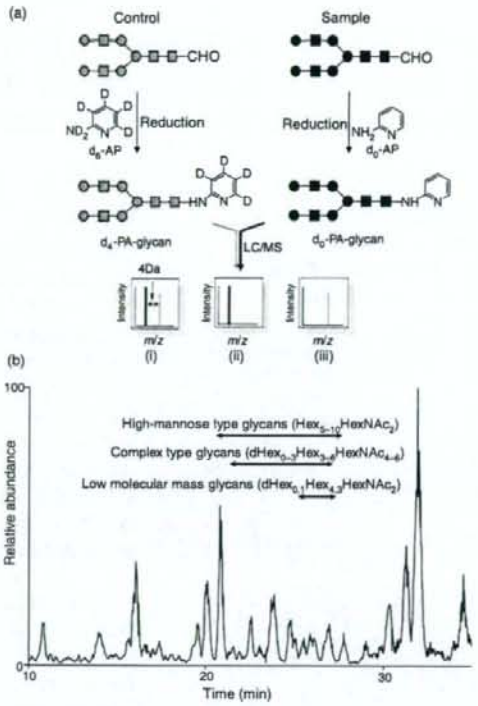

Figure 1. (a) Quantitative glycan profiling using the stable isotope-tagging method and liquid chromatography/mass spectrometry (LC/MS). (i) sample = control, (ii) sample > control, (iii) sample < control. (b) Total ion chromatogram obtained by a single scan (m/z 700–2000) of the d_0-glycan and d_4-glycan mixture.

Rokko, was purchased from Daiwa Kasei (Shiga, Japan). Glycopeptidase A (PNGase A) was obtained from Seikagaku Kogyo Corporation (Tokyo, Japan). Non-deuterium-labelled 2-aminopyridine (d_0-AP) and deuterium-labelled 2-aminopyridine (d_6-AP) were purchased from Takara Bio (Otsu, Japan) and Cambridge Isotope Laboratories (Andover, MA), respectively.

Sample preparation

Mouse kidneys were filtered using a cell strainer (70 μm; BD Biosciences, San Jose, CA) and contaminating blood cells in the kidney cells were burst in 140 mM NH_4Cl–Tris buffer (pH 7·2). The surviving kidney cells were washed three times with phosphate-buffered saline containing a mixture of protease inhibitors (Wako, Tokyo, Japan) and dissolved in guanidine–HCl buffer (8 M guanidine–HCl, 0·5 M Tris–HCl, pH 8·6) containing a mixture of protease inhibitors by vortexing at 4°. The protein concentration was measured using a 2-D Quant Kit (GE Healthcare

Bio-Sciences, Uppsala, Sweden). The protein solution (200 μg proteins) was incubated with 40 mM dithiothreitol at 65° for 30 min. Freshly prepared sodium iodoacetate (final concentration, 96 mM) was added to the sample solution, and the mixture was incubated at room temperature for 40 min in the dark. The reaction was stopped by adding cystine (6 mg/ml in 2 M HCl) in an amount equal to the amount of dithiothreitol. The solution containing carboxymethylated proteins was diluted in four times its volume of H_2O, and the mixture was incubated with 0·1 μg of thermolysin at 65° for 1 hr. After terminating the reaction by boiling, the reaction mixture was diluted in four times its volume of 0·2 M acetate buffer. The *N*-linked glycans were released by treatment with PNGase A (1 mU) at 37° for 16 hr and were desalted using an EnviCarb C cartridge (Supelco, Bellefonte, PA).

Labelling of N-glycans with d_0-AP and d_6-AP

Glycans released from the SLE-model mouse cells were incubated in acetic acid (20 μl) with 12·5 M d_0-AP at 90° for 1 hr. Next, 3·3 M borane–dimethylamine complex reducing reagent in acetic acid (20 μl) was added to the solution and the mixture was incubated at 80° for 1 hr. Excess reagent was removed by evaporation, and d_0-PA glycans were desalted using an EnviCarb C cartridge, concentrated in a SpeedVac and reconstituted in 20 μl of 5 mM ammonium acetate (pH 9·6). Glycans released from the control mouse were labelled with d_6-AP in a similar manner. The resulting d_4-PA glycans were combined with d_0-PA glycans, which were prepared from an equal amount of proteins.

On-line liquid chromatography/mass spectrometry

The sample solution (4 μl) was injected into the LC/MS system through a 5-μl capillary loop. The d_0-PA and d_4-PA glycans were separated in a graphitized carbon column (Hypercarb, 150 × 0·2 mm, 5 μm; Thermo Fisher Scientific, Waltham, MA) at a flow rate of 2 μl/min in a Magic 2002 LC system (Michrom Bioresources, Auburn, CA). The mobile phases were 5 mM ammonium acetate containing 2% acetonitrile (pH 9·6, A buffer) and 5 mM ammonium acetate containing 90% acetonitrile (pH 9·6, B buffer). The PA-glycans were eluted with a linear gradient of 5–45% of B buffer for 90 min.

Mass spectrometric analysis of PA glycans was performed using a Fourier transform ion cyclotron resonance/ion trap mass spectrometer (FT-ICR-MS, LTQ-FT; Thermo Fisher Scientific) equipped with a nanoelectrospray ion source (AMR, Tokyo, Japan). For MS, the electrospray voltage was 2·0 kV in the positive ion mode, the capillary temperature was 200°, the collision energy was 25% for MS^n experiment, and the maximum injection times for FT-ICR-MS and MS^n were 1250 and 50 milliseconds, respectively. The resolution of FT-ICR-MS was 50 000, the scan time (*m/z* 700–2000) was approximately 0·2 seconds, dynamic exclusion was 18 seconds, and the isolation width was 3·0 U (range of precursor ions ± 1·5).

Results

Quantitative profiling of kidney oligosaccharides in the SLE-model mouse

The recovery of oligosaccharides from whole tissues and cells is generally low because of the insolubility of the membrane fraction and possible degradation of the glycans. To improve the recovery of *N*-glycans from kidney cells, whole cells were dissolved in guanidine hydrochloride solution, and all proteins, including membrane proteins, were digested into peptides and glycopeptides with thermolysin. The *N*-glycans were then released from the glycopeptides with PNGase A, which is capable of liberating *N*-linked oligosaccharides even at the N- and/or C-terminals of peptides. The *N*-linked oligosaccharides from the SLE-model mice and control mice were labelled with d_0-AP and d_6-AP, respectively. The mixture of labelled glycans derived from an equal amount of proteins was subjected to quantitative glycan profiling using LC/MS^n.

Figure 1(b) shows the total ion chromatogram obtained by a single mass scan (*m/z* 700–2000) of the glycan mixture in the positive ion mode. Although the MS data contain many MS spectra derived from contaminating low-molecular-weight peptides, the MS/MS spectra of oligosaccharides could be sorted based on the existence of carbohydrate-distinctive ions, such as $HexHexNAc^+$ (*m/z* 366) and $Hex(dHex)HexNAc^+$ (*m/z* 512). The monosaccharide compositions of the precursor ions were calculated from accurate *m/z* values acquired by FT-ICR-MS. Oligosaccharides found at 25–27 min were assigned to low-molecular-mass glycans consisting of $dHex_{0,1}Hex_{4,3}HexNAc_2$ (dHex, deoxyhexose; Hex, hexose; HexNAc, *N*-acetylhexosamine). High-mannose-type glycans, which consist of $Hex_{5-10}HexNAc_2$, were located at 20–28 min; complex-type glycans ($dHex_{0-3}Hex_{3-6}HexNAc_{4-6}$) were found at 21–27 min. Figure 2(a) shows the relative intensities of the molecular ions of *N*-glycans in the SLE-model mouse, which may correspond roughly to the levels of individual *N*-glycans. More than half of all glycans were complex-type oligosaccharides, and the most prominent glycan was $dHex_3Hex_5HexNAc_5$. Man-9 ($Hex_9HexNAc_2$) was the second most common oligosaccharide. Nearly one-quarter of the glycans were low-molecular-mass glycans, and $dHex_1Hex_2HexNAc_2$ was the third most abundant glycan in the SLE-model mouse. The rate of percentage change in individual glycans between the SLE-model mice and control mice was calculated from the intensity ratio of d_0-glycan and d_4-glycan

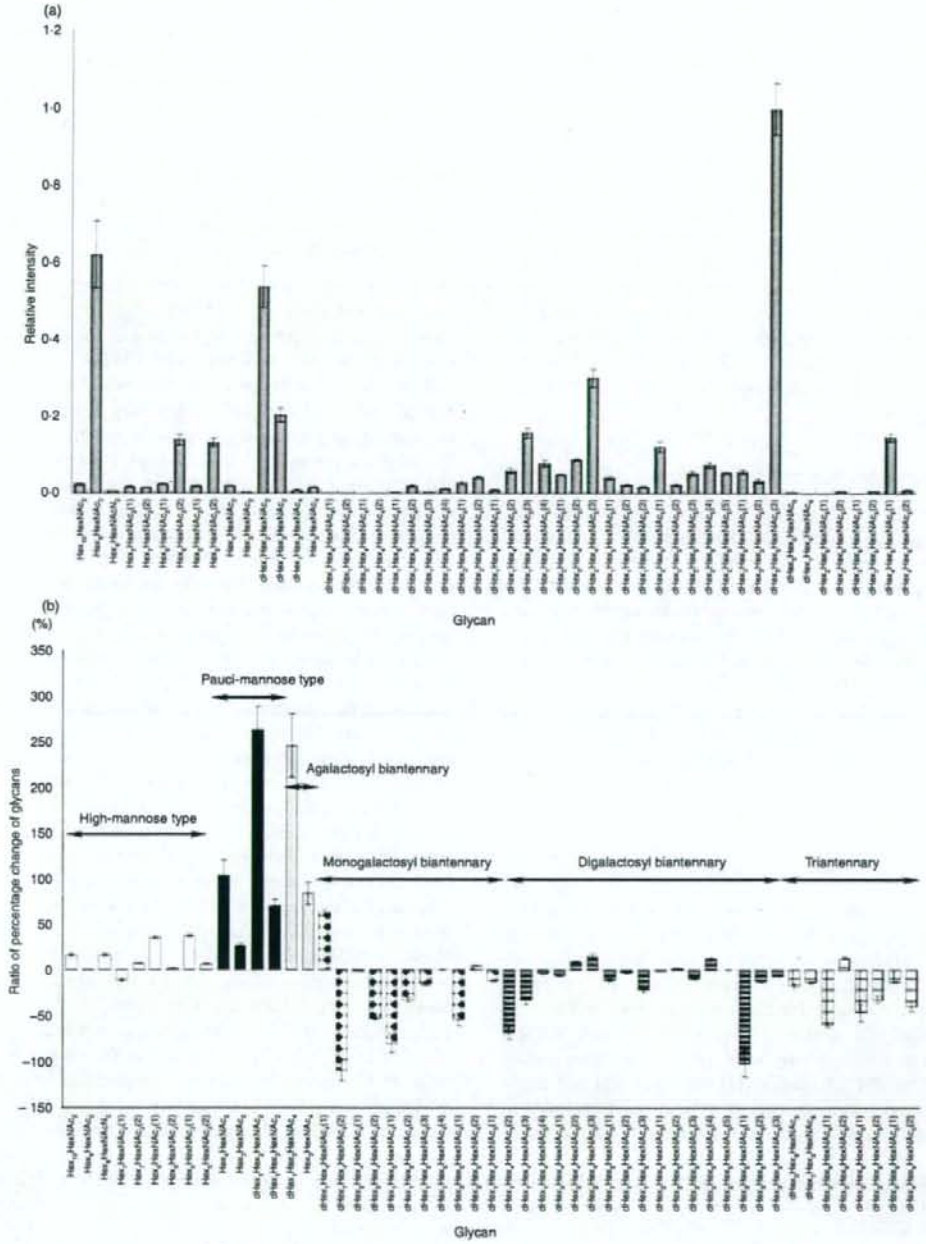

Figure 2. (a) Relative intensities of the molecular ions of d_0-pyridyl amino (PA) glycans from the systemic lupus erythematosus (SLE) model mouse. The intensity of the most intense ion ($[M + 2H]^{2+}$of d_4-PA $dHex_3Hex_3HexNAc_3(3)$, *m/z* 1180·97) was taken as 1·0. (b) Rate of percentage change of d_0/d_4-glycans. Each value is the average of three biological repeats. Error bars correspond to the standard deviation. The numbers in parentheses show the isomers.

molecular ions (Fig. 2b). The significant changes found in many glycans are described below.

Increased oligosaccharides in the SLE-model mouse

Figure 3(a,b) show the mass and MS/MS spectra of the most increased glycan, which showed a notable increase in the SLE-model mouse. Based on *m/z* values of molecular ions and differences of 1·00 U in *m/z* values among monoisotopic ions, the intense ion (*m/z* 973·40) and its neighbour ion (*m/z* 977·43) were assigned to $[M+H]^+$ of d_0-PA $dHex_1Hex_3HexNAc_2$, and d_4-PA $dHex_1Hex_3HexNAc_2$, respectively (Fig. 3a). The intensity ratio of these ions suggested that the level of $dHex_1Hex_3HexNAc_2$ increased 3·6-fold in the SLE-model mouse. The structure of this oligosaccharide was estimated to be a core-fucosylated trimannosyl core lacking a Man residue from the successive cleavages of Man (Y_3: *m/z* 815), Man (Y_2: *m/z* 653), GlcNAc (Y_1: *m/z* 450) and Fuc ($Y_{1/1'}$: *m/z* 304) (inset in Fig. 3b). Such a defective *N*-glycan is known as a paucimannose-type glycan, and is rarely found in vertebrates. All paucimannose-type glycans, such as $dHex_1Hex_3HexNAc_2$ (a core-fucosylated trimannosyl core) and $Hex_3HexNAc_2$ (a non-fucosylated trimannosyl core) were increased in the SLE-model mouse. Furthermore, a two-fold increase was found in $Hex_4HexNAc_2$ (Man-4).

Figure 4 shows the molecular ratios of individual *N*-glycans between the SLE-model mice and control mice. A remarkable increase (3·5-fold) was also found in $dHex_1Hex_3HexNAc_4$, which is assigned to a core-fucosylated biantennary oligosaccharide lacking two non-reducing terminal Gal residues; its non-fucosylated form ($Hex_3HexNAc_4$) was also increased 1·8-fold in the SLE-model mouse. In other complex-type glycans, $dHex_1Hex_4HexNAc_4$ (1), which is assigned to a biantennary oligosaccharide lacking one molecule of Gal, increased 1·6-fold. Interestingly, a significant decrease was found in $dHex_1Hex_4HexNAc_4$ (2), a positional isomer of $dHex_1Hex_4HexNAc_4$ (1); this might have been caused by galactosylation on either GlcNAc-Manα1–3 or GlcNAc-Manα1–6. In contrast, no change was found between fucosylated and non-fucosylated oligosaccharides, nor between bisected and non-bisected oligosaccharides.

A significant increase was found in some high-mannose-type oligosaccharides, such as $Hex_5HexNAc_2$ (Man-5; + 137%) and $Hex_6HexNAc_2$ (1) (Man-6; + 136%), while $Hex_7HexNAc_2$ (1,2) (Man-7) and a positional isomer of $Hex_6HexNAc_2$ (1) [$Hex_6HexNAc_2$ (2)] remained unchanged in the SLE-model mouse. A slight increase was found in $Hex_8HexNAc_2$ (Man-8; + 116%) and $Hex_{10}HexNAc_2$ (possibly assigned to Man-9 plus Glc; + 116%).

Decreased oligosaccharides in the SLE-model mouse

The mass spectrum of the most decreased glycan is shown in Fig. 5(a). Based on differences of 0·5 U in *m/z* values among monoisotopic ions, molecular ions at *m/z* 1180·97

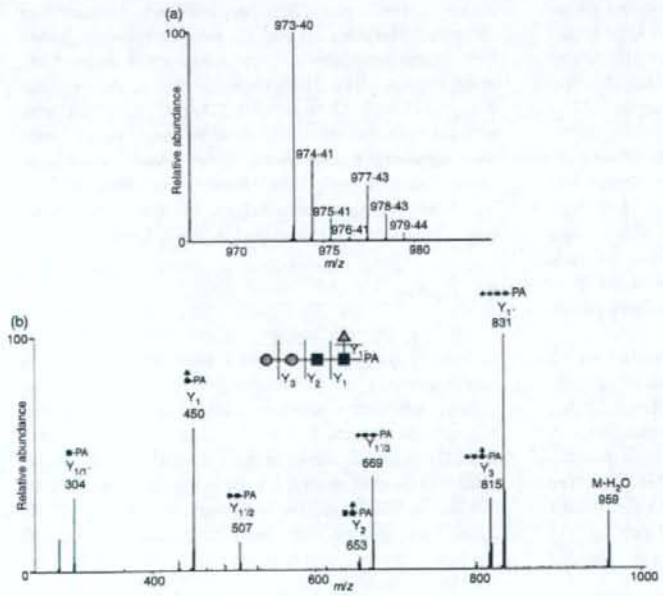

Figure 3. Mass (a) and mass spectrometry (MS)/MS (b) spectra of the most increased glycan ($dHex_1Hex_3HexNAc_2$). Precursor ion, *m/z* 973·4; grey circle, mannose; grey triangle, fucose; black square, *N*-acetylglucosamine.

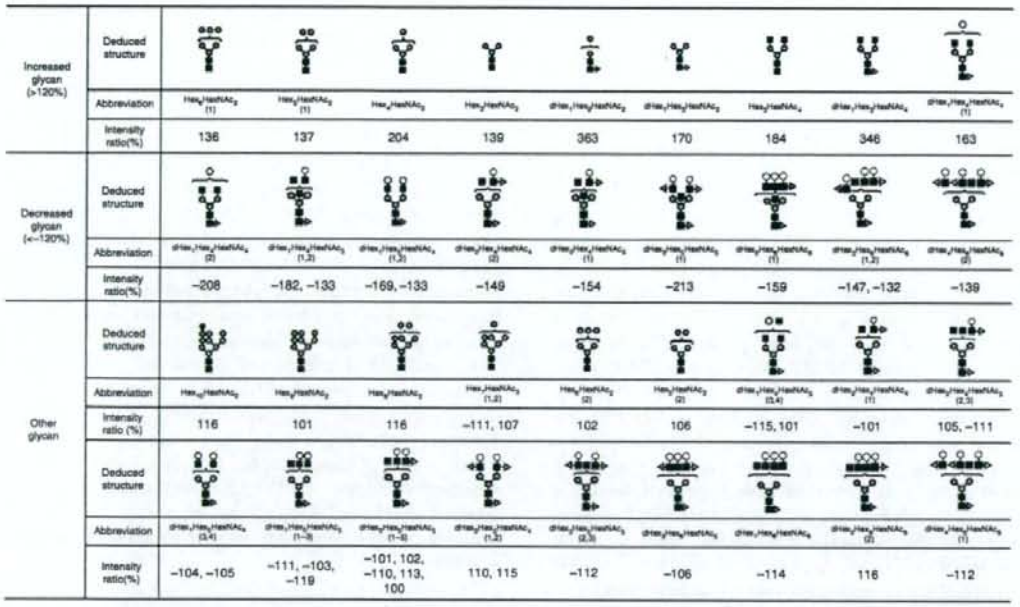

Figure 4. Summary of quantitative analysis of the systemic lupus erythematosus (SLE) model mouse against control mice. Values of relative ratios are the averages of three biological repeats. Grey circle, mannose; white circle, galactose; grey triangle, fucose; black square, *N*-acetylglucosamine.

and 1182·98 are estimated to be $[M + 2H]^{2+}$ of d_0-PA and d_4-PA $dHex_3Hex_5HexNAc_5$ (1), respectively. The intensity ratio of $d_0 : d_4$ glycans suggests that this glycan in the SLE-model mouse was decreased to 47% of the amount found in the control mouse. Figure 5(b) shows the MS^{2-4} spectra of d_0-PA $dHex_3Hex_5HexNAc_5$ (1) (precursor ion, *m/z* 1180·97). The fragment ion at *m/z* 512 in MS/MS (i) and MS/MS/MS (ii) spectra, which corresponds to $dHex_1Hex_1HexNAc_1^+$, suggests the attachment of two Lewis motifs on the side chains of the glycan. The presence of $dHex_1HexNAc_1PA^+$ (*m/z* 446) and $dHex_1Hex_1HexNAc_3PA^+$ (*m/z* 1015) reveals the linkages of a core fucose and a bisecting GlcNAc. Based on these fragments, this decreased glycan is estimated to be a Lewis-motif-modified, core-fucosylated and bisected biantennary oligosaccharide (inset in Fig. 5).

As shown in Figs 2(b) and 4, oligosaccharides lacking one molecule of Gal with and without bisecting GlcNAc [$dHex_1Hex_4HexNAc_4$ (2) and $dHex_1Hex_4HexNAc_5$ (1)] were decreased to 48% and 55%, respectively. A significant decrease was also found in other monogalactobiantennary oligosaccharides, such as $dHex_2Hex_4HexNAc_4$ (2) (a Lewis-motif-modified, core-fucosylated monogalacto-biantennary) and $dHex_2Hex_4HexNAc_5$ (1) (a Lewis-motif-modified core-fucosylated and bisected monogalacto-biantennary).

The oligosaccharides, non-reducing ends of which are fully galactosylated, were decreased in the SLE-model mouse. For example, monofucosyl biantennary $dHex_1Hex_5HexNAc_4$ (1) and (2) were decreased 59% and 75%, respectively. The di-, tri- and tetra-fucosylated oligosaccharides, $dHex_2Hex_6HexNAc_6$ (1), $dHex_3Hex_6HexNAc_6$ (1,2) and $dHex_4Hex_6HexNAc_6$ (1,2), which were estimated to be tri- and tetraantennary forms, were also significantly decreased. These results show that oligosaccharides with a complicated structure, such as high branching oligosaccharides and di- and tri-fucosylated oligosaccharides, were decreased in the SLE-model mouse.

Discussion

Using the isotope-tagging method, we demonstrated aberrant *N*-glycosylation on the kidney proteins of a SLE-model mouse. We found increases in low-molecular-mass glycans with simple structures, including paucimannose-type glycans, agalacto-biantennary oligosaccharides, Man-5 and Man-6, and decreases in glycans which have a complicated and diverse structure, such as digalacto-biantennary oligosaccharides and highly fucosylated glycans (Fig. 4). An increase in agalacto-biantennary oligosaccharides on IgG has been reported in the sera of patients with autoimmune diseases, including SLE, rheumatoid arthritis and IgA

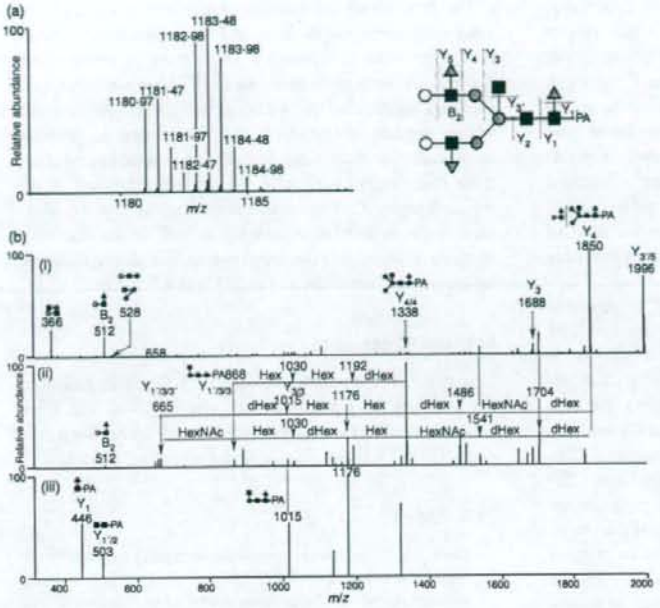

Figure 5. (a) Mass spectrum of the most decreased glycan [$dHex_3Hex_5HexNAc_5$ (1)]; (b-i) Mass spectrometry (MS)/MS spectrum of *m/z* 1181·0; (b-ii) MS/MS/MS spectrum of *m/z* 1849·7; (b-iii) MS/MS/MS/MS spectrum of *m/z* 1338·3. Grey circle, mannose; white circle, galactose; grey triangle, fucose; black square, *N*-acetylglucosamine; dHex, deoxyhexose (fucose); Hex, hexose (mannose and galactose); HN, *N*-acetylhexosamine (*N*-acetylglucosamine).

nephropathy.[9,11,28] The present findings show that abnormal glycosylation occurs not only in IgG in serum but also in several glycoproteins in the SLE-model mouse kidney.

Figure 6 shows the biosynthesis pathway of *N*-linked oligosaccharides in mammalian cells. Man-9, a product in the early stage of the pathway, is processed to Man-5 in the endoplasmic reticulum, and a GlcNAc and Fuc are added to Man-5 in the Golgi apparatus. After the removal of two Man residues by αM-II, GlcNAc, Gal and Fuc are further added to oligosaccharides by several glycosyltransferases. There have been a few reports on paucimannose-type oligosaccharides in vertebrates;[29] however, these glycans are common oligosaccharides in other multicellular organisms such as insects and *Caenorhabditis elegans*.[30,31] The membrane protease β-*N*-acetylglucosaminidase is thought to mediate the synthesis of paucimannose-type oligosaccharides.[32] Based on core fucosylation on some paucimannose-type oligosaccharides, it was deduced that β-*N*-acetylglucosaminidase might act on glycan synthesis after *N*-acetylglucosaminyltransferase I, core fucosyltransferase and αM-II.[32] The synthesis of paucimannose-type oligosaccharides may be involved in the suppression of growing diversity and complexity of glycan structures.

We found a number of changes in the levels of monogalacto-biantennary oligosaccharides in the SLE mouse. Galactosylation to agalacto-biantennary oligosaccharides is mediated by β-1,4-galactosyltransferase

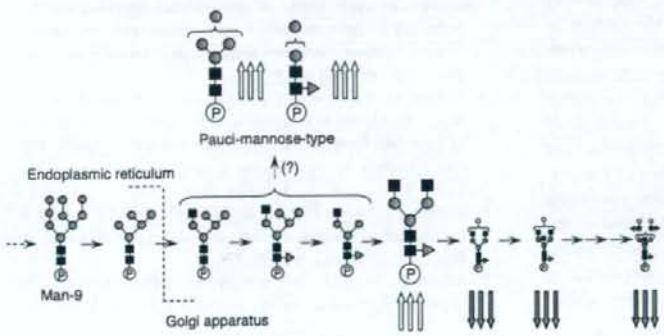

Figure 6. Biosynthesis pathway of *N*-linked oligosaccharides in mammalian cells. Triple up-arrow, increases of more than +2·0; triple down-arrow, decreases of not more than −2·0. Grey circle, mannose; white circle, galactose; grey triangle, fucose; black square, *N*-acetylglucosamine. 'P' is protein portion.

(β-1,4-GalTase).[33] Previous studies suggested that translational repression of β-1,4-GalTase in lymphocytes is associated with an increase in agalacto-oligosaccharides on IgG in the serum of the MRL-lpr mouse.[34] Although the activity of β-1,4-GalTase remains unknown in the SLE-model mouse, the increase in agalacto forms and the decrease in digalacto forms imply changes in β-1,4-GalTase activity. The present results suggest a decrease in diverse and complex glycans, which are synthesized at a late stage in the *N*-glycan synthesis pathway, and an increase in the simple glycans appearing at an early stage in the SLE-model mouse.

The activation of complements is involved in glomerular nephritis of SLE.[35–37] The complements are activated through three pathways: a classical pathway, an alternative pathway and a lectin pathway. In the classical pathway, a binding of C1q to an immune complex triggers the activation of C1r and C1s. Activated C1s cleaves C4 and C2, generating C3 convertase (C4b2a), which generates C3b. The complement component subsequently produces C5b-9 complex, which leads to an inflammatory response on host tissues.[38–41] The excess deposition of immune complexes followed by a sustained immune response triggers tissue disorders, including lupus nephritis.[42–45] In the lectin pathway, mannose-binding lectin (MBL) is associated with the activation of complements. Two forms of MBL (MBL-A and MBL-C) are present in complexes with MBL-associated serine proteases (MASPs) in mice. The MASPs are activated by binding MBL to Man or GlcNAc on the surface of the antigen in a calcium-dependent manner.[46–49] Like C1s in the classical pathway, activated MASPs cleave C4 and C2.[50,51] In lupus nephritis, MBL-A and MBL-C in the immune complex bind to GlcNAc residues at the reducing ends of agalacto-biantennary oligosaccharides in IgG,[52] and subsequently activate the complements.[53,54] In αM-II-deficient mice, which suffer from SLE-like syndromes including kidney disorders, the majority of glycans are hybrid-type oligosaccharides because of the failure of Man trimming by the lack of αM-II.[16] Green *et al.* concluded that MBL recognized Manα1–3 and Manα1–6 linkages in hybrid-type oligosaccharides,[17] and glycans lacking normal side chains, including agalacto-biantennary oligosaccharides, might be involved in the aberrant immune response in autoimmune diseases. Paucimannose glycans, which contain exposed Manα1–3 or Manα1–6 linkages, may be recognized as ligand carbohydrates by MBL. Our present finding, an increase in paucimannose oligosaccharides and agalacto forms, might result from an alteration of the biosynthesis pathway of *N*-glycans. The alterations may cause the aberrant glycosylations on most of the glycoproteins rather than some glycoproteins in the SLE-model mouse. The changes in glycosylation might be involved in an autoimmune pathogenesis in the SLE-model mouse kidney.

The continuous production of aberrant antibodies that react with components from self-tissue and accumulation in the immune complex are thought to promote tissue damage in autoimmune disease.[55,56] The mechanism of localized accumulation in the immune complex in some tissues remains unknown in SLE. We found an increase in glycans that may bind to MBL and subsequently promote complement activation via the lectin pathway in the mouse kidney. Our present results suggest that an aberrant *N*-glycan synthesis pathway as well as an abnormal immune system may be involved in the damage caused by glomerular nephritis in the SLE-model mouse.

Acknowledgements

This study was supported in part by a Grant-in-Aid from the Ministry of Health, Labor, and Welfare, and Core Research for the Evolutional Science and Technology Program (CREST), Japan Science and Technology Corp (JST).

References

1 Dwek RA. Glycobiology: toward understanding the function of sugars. *Chem Rev* 1996; **96**:683–720.
2 Helenius A, Aebi M. Intracellular functions of N-linked glycans. *Science* 2001; **291**:2364–9.
3 Zak I, Lewandowska E, Gnyp W. Selectin glycoprotein ligands. *Acta Biochim Pol* 2000; **47**:393–412.
4 Axford JS. Glycosylation and rheumatic disease. *Biochim Biophys Acta* 1999; **1455**:219–29.
5 Feizi T, Gooi HC, Childs RA, Picard JK, Uemura K, Loomes LM, Thorpe SJ, Hounsell EF. Tumour-associated and differentiation antigens on the carbohydrate moieties of mucin-type glycoproteins. *Biochem Soc Trans* 1984; **12**:591–6.
6 Kannagi R, Izawa M, Koike T, Miyazaki K, Kimura N. Carbohydrate-mediated cell adhesion in cancer metastasis and angiogenesis. *Cancer Sci* 2004; **95**:377–84.
7 Goodarzi MT, Turner GA. Decreased branching, increased fucosylation and changed sialylation of alpha-1-proteinase inhibitor in breast and ovarian cancer. *Clin Chim Acta* 1995; **236**:161–71.
8 Yamashita K, Fukushima K, Sakiyama T, Murata F, Kuroki M, Matsuoka Y. Expression of Sia alpha 2→6Gal beta 1→4GlcNAc residues on sugar chains of glycoproteins including carcinoembryonic antigens in human colon adenocarcinoma: applications of *Trichosanthes japonica* agglutinin I for early diagnosis. *Cancer Res* 1995; **55**:1675–9.
9 Tomana M, Schrohenloher RE, Reveille JD, Arnett FC, Koopman WJ. Abnormal galactosylation of serum IgG in patients with systemic lupus erythematosus and members of families with high frequency of autoimmune diseases. *Rheumatol Int* 1992; **12**:191–4.
10 Mizuochi T, Hamako J, Nose M, Titani K. Structural changes in the oligosaccharide chains of IgG in autoimmune MRL/Mp-lpr/lpr mice. *J Immunol* 1990; **145**:1794–8.
11 Arnold JN, Wormald MR, Sim RB, Rudd PM, Dwek RA. The impact of glycosylation on the biological function and structure

of human immunoglobulins. *Annu Rev Immunol* 2007; **25**:21–50.

12 Das H, Atsumi T, Fukushima Y *et al.* Diagnostic value of anti-agalactosyl IgG antibodies in rheumatoid arthritis. *Clin Rheumatol* 2004; **23**:218–22.

13 Raghav SK, Gupta B, Agrawal C, Saroha A, Das RH, Chaturvedi VP, Das HR. Altered expression and glycosylation of plasma proteins in rheumatoid arthritis. *Glycoconj J* 2006; **23**:167–73.

14 Elliott MA, Elliott HG, Gallagher K, McGuire J, Field M, Smith KD. Investigation into the concanavalin A reactivity, fucosylation and oligosaccharide microheterogeneity of alpha 1-acid glycoprotein expressed in the sera of patients with rheumatoid arthritis. *J Chromatogr B Biomed Sci Appl* 1997; **688**:229–37.

15 Rops AL, van den Hoven MJ, Bakker MA *et al.* Expression of glomerular heparan sulphate domains in murine and human lupus nephritis. *Nephrol Dial Transplant* 2007; **22**:1891–902.

16 Chui D, Sellakumar G, Green R *et al.* Genetic remodeling of protein glycosylation *in vivo* induces autoimmune disease. *Proc Natl Acad Sci USA* 2001; **98**:1142–7.

17 Green RS, Stone EL, Tenno M, Lehtonen E, Farquhar MG, Marth JD. Mammalian *N*-glycan branching protects against innate immune self-recognition and inflammation in autoimmune disease pathogenesis. *Immunity* 2007; **27**:308–20.

18 Wada Y. Mass spectrometry in the detection and diagnosis of congenital disorders of glycosylation. *Eur J Mass Spectrom (Chichester, Eng)* 2007; **13**:101–3.

19 Faid V, Chirat F, Seta N, Foulquier F, Morelle W. A rapid mass spectrometric strategy for the characterization of *N*- and *O*-glycan chains in the diagnosis of defects in glycan biosynthesis. *Proteomics* 2007; 7:1800–13.

20 Miyamoto S. Clinical applications of glycomic approaches for the detection of cancer and other diseases. *Curr Opin Mol Ther* 2006; **8**:507–13.

21 Yuan J, Hashii N, Kawasaki N, Itoh S, Kawanishi T, Hayakawa T. Isotope tag method for quantitative analysis of carbohydrates by liquid chromatography-mass spectrometry. *J Chromatogr A* 2005; **1067**:145–52.

22 Alvarez-Manilla G, Warren NL, Abney T, Atwood J III, Azadi P, York WS, Pierce M, Orlando R. Tools for glycomics: relative quantitation of glycans by isotopic permethylation using 13CH3I. *Glycobiology* 2007; **17**:677–87.

23 Kang P, Mechref Y, Kyselova Z, Goetz JA, Novotny MV. Comparative glycomic mapping through quantitative permethylation and stable-isotope labeling. *Anal Chem* 2007; **79**:6064–73.

24 Bowman MJ, Zaia J. Tags for the stable isotopic labeling of carbohydrates and quantitative analysis by mass spectrometry. *Anal Chem* 2007; **79**:5777–84.

25 Watanabe-Fukunaga R, Brannan CI, Copeland NG, Jenkins NA, Nagata S. Lymphoproliferation disorder in mice explained by defects in Fas antigen that mediates apoptosis. *Nature* 1992; **356**:314–7.

26 Adachi M, Watanabe-Fukunaga R, Nagata S. Aberrant transcription caused by the insertion of an early transposable element in an intron of the Fas antigen gene of lpr mice. *Proc Natl Acad Sci USA* 1993; **90**:1756–60.

27 Merino R, Iwamoto M, Fossati L, Izui S. Polyclonal B cell activation arises from different mechanisms in lupus-prone (NZB × NZW)F_1 and MRL/MpJ-lpr/lpr mice. *J Immunol* 1993; **151**:6509–16.

28 Homma H, Tozawa K, Yasui T, Itoh Y, Hayashi Y, Kohri K. Abnormal glycosylation of serum IgG in patients with IgA nephropathy. *Clin Exp Nephrol* 2006; **10**:180–5.

29 Hase S, Okawa K, Ikenaka T. Identification of the trimannosylchitobiose structure in sugar moieties of Japanese quail ovomucoid. *J Biochem* 1982; **91**:735–7.

30 Kubelka V, Altmann F, Kornfeld G, Marz L. Structures of the N-linked oligosaccharides of the membrane glycoproteins from three lepidopteran cell lines (Sf-21, IZD-Mb-0503, Bm-N). *Arch Biochem Biophys* 1994; **308**:148–57.

31 Natsuka S, Adachi J, Kawaguchi M, Nakakita S, Hase S, Ichikawa A, Ikura K. Structural analysis of N-linked glycans in *Caenorhabditis elegans*. *J Biochem* 2002; **131**:807–13.

32 Altmann F, Schwihla H, Staudacher E, Glossl J, Marz L. Insect cells contain an unusual, membrane-bound beta-*N*-acetylglucosaminidase probably involved in the processing of protein *N*-glycans. *J Biol Chem* 1995; **270**:17344–9.

33 Guo S, Sato T, Shirane K, Furukawa K. Galactosylation of N-linked oligosaccharides by human beta-1,4-galactosyltransferases I, II, III, IV, V, and VI expressed in Sf-9 cells. *Glycobiology* 2001; **11**:813–20.

34 Jeddi PA, Lund T, Bodman KB *et al.* Reduced galactosyltransferase mRNA levels are associated with the agalactosyl IgG found in arthritis-prone MRL-lpr/lpr strain mice. *Immunology* 1994; **83**:484–8.

35 Cameron JS. Lupus nephritis. *J Am Soc Nephrol* 1999; **10**:413–24.

36 Walport MJ. Complement. First of two parts. *N Engl J Med* 2001; **344**:1058–66.

37 Walport MJ. Complement. Second of two parts. *N Engl J Med* 2001; **344**:1140–4.

38 Botto M. Links between complement deficiency and apoptosis. *Arthritis Res* 2001; **3**:207–10.

39 Hanayama R, Tanaka M, Miyasaka K, Aozasa K, Koike M, Uchiyama Y, Nagata S. Autoimmune disease and impaired uptake of apoptotic cells in MFG-E8-deficient mice. *Science* 2004; **304**:1147–50.

40 Arason GJ, Steinsson K, Kolka R, Vikingsdottir T, D'Ambrogio MS, Valdimarsson H. Patients with systemic lupus erythematosus are deficient in complement-dependent prevention of immune precipitation. *Rheumatology (Oxford)* 2004; **43**:783–9.

41 Cook HT, Botto M. Mechanisms of disease: the complement system and the pathogenesis of systemic lupus erythematosus. *Nat Clin Pract Rheumatol* 2006; **2**:330–7.

42 Gunnarsson I, Sundelin B, Heimburger M, Forslid J, van Vollenhoven R, Lundberg I, Jacobson SH. Repeated renal biopsy in proliferative lupus nephritis – predictive role of serum C1q and albuminuria. *J Rheumatol* 2002; **29**:693–9.

43 Buyon JP, Tamerius J, Belmont HM, Abramson SB. Assessment of disease activity and impending flare in patients with systemic lupus erythematosus. Comparison of the use of complement split products and conventional measurements of complement. *Arthritis Rheum* 1992; **35**:1028–37.

44 Markiewski MM, Lambris JD. The role of complement in inflammatory diseases from behind the scenes into the spotlight. *Am J Pathol* 2007; **171**:715–27.

45 Sturfelt G. The complement system in systemic lupus erythematosus. *Scand J Rheumatol* 2002; **31**:129–32.

46 Holmskov U, Malhotra R, Sim RB, Jensenius JC. Collectins: collagenous C-type lectins of the innate immune defense system. *Immunol Today* 1994; **15**:67–74.

47 Weis WI, Drickamer K, Hendrickson WA. Structure of a C-type mannose-binding protein complexed with an oligosaccharide. *Nature* 1992; **360**:127–34.

48 Takahashi M, Mori S, Shigeta S, Fujita T. Role of MBL-associated serine protease (MASP) on activation of the lectin complement pathway. *Adv Exp Med Biol* 2007; **598**:93–104.

49 Turner MW. Mannose-binding lectin: the pluripotent molecule of the innate immune system. *Immunol Today* 1996; **17**:532–40.

50 Holmskov U, Malhotra R, Sim RB, Jensenius JC. Collectins: collagenous C-type lectins of the innate immune defense system. *Immunol Today* 1994; **15**:67–74.

51 Thiel S, Vorup-Jensen T, Stover CM *et al.* A second serine protease associated with mannan-binding lectin that activates complement. *Nature* 1997; **386**:506–10.

52 Lhotta K, Wurzner R, Konig P. Glomerular deposition of mannose-binding lectin in human glomerulonephritis. *Nephrol Dial Transplant* 1999; **14**:881–6.

53 Ohsawa I, Ohi H, Tamano M *et al.* Cryoprecipitate of patients with cryoglobulinemic glomerulonephritis contains molecules of the lectin complement pathway. *Clin Immunol* 2001; **101**:59–66.

54 Trouw LA, Seelen MA, Duijs JM *et al.* Activation of the lectin pathway in murine lupus nephritis. *Mol Immunol* 2005; **42**:731–40.

55 Jorgensen TN, Gubbels MR, Kotzin BL. New insights into disease pathogenesis from mouse lupus genetics. *Curr Opin Immunol* 2004; **16**:787–93.

56 Lauwerys BR, Wakeland EK. Genetics of lupus nephritis. *Lupus* 2005; **14**:2–12.

Journal of Chromatography B, 869 (2008) 20–30

Contents lists available at ScienceDirect

Journal of Chromatography B

journal homepage: www.elsevier.com/locate/chromb

Simultaneous glycosylation analysis of human serum glycoproteins by high-performance liquid chromatography/tandem mass spectrometry

Akira Harazono[a,*], Nana Kawasaki[a,b], Satsuki Itoh[a], Noritaka Hashii[a], Yukari Matsuishi-Nakajima[a,b], Toru Kawanishi[a], Teruhide Yamaguchi[a]

[a] Division of Biological Chemistry and Biologicals, National Institute of Health Sciences, 1-18-1 Kami-yoga, Setagaya-Ku, Tokyo 158-8501, Japan
[b] Core Research for Evolutional Science and Technology (CREST) of Japan Science and Technology Agency (JST), Kawaguchi Center Building, 4-1-8 Hon-cho, Kawaguchi, Saitama 332-0012, Japan

ARTICLE INFO

Article history:
Received 19 December 2007
Accepted 5 May 2008
Available online 10 May 2008

Keywords:
Glycosylation analysis
Human serum
Glycopeptide
LC/MS
LC/MS/MS
Immunoglobulin G
Haptoglobin
Transferrin
Ceruloplasmin

ABSTRACT

Changes in the glycosylation of some serum proteins are associated with certain diseases. In this study, we performed simultaneous site-specific glycosylation analysis of abundant serum glycoproteins by LC/Qq-TOF MS of human serum tryptic digest, the albumin of which was depleted. The glycopeptide peaks on the chromatogram were basically assigned by database searching with modified peak-list text files of MS/MS spectra and then based on mass differences of glycan units from characterized glycopeptides. Glycopeptide of IgG, haptoglobin and ceruloplasmin were confirmed by means of a comparison of their retention times and *m/z* values with those obtained by LC/MS of commercially available glycoproteins. Mass spectrometric carbohydrate heterogeneity in the assigned glycopeptides was analyzed by an additional LC/MS. We successfully demonstrated site-specific glycosylation of 23 sites in abundant serum glycoproteins.

1. Introduction

Glycosylation of proteins is a common post-translational modification of proteins [1], and most proteins in serum are glycosylated [2]. Changes in the oligosaccharide moieties of certain serum glycoproteins are associated with human diseases. Oligosaccharides lacking galactose residues in immunoglobulin G (IgG) are increased in rheumatoid arthritis [3,4] and Crohn's syndrome [5]. Congenital disorders of glycosylation (CDG) are genetic disorders in the N-linked glycosylation processing pathway [6], and can be diagnosed by glycosylation analysis of serum glycoproteins [7], such as transferrin and haptoglobin. Significant increases in fucose levels and oligosaccharide branches in haptoglobin have been found to be associated with ovarian cancer [8,9], lung cancer [10–12], pancreatic cancer [13] and hepatocellular carcinoma [14]. Changes in glycosylation are also found in acute-phase proteins, such as alpha-1-acid glycoprotein and ceruloplasmin, in lung cancer [15]. These findings suggest the potential of the glycosylation analysis of serum glycoproteins in diagnosis of some diseases and an investigation of new biomarkers. At present the glycosylation of each protein is examined individually, therefore simultaneous analysis of serum glycoproteins has been required for rapid diagnosis with a limited amount of sample.

Mass spectrometry (MS) is known as a powerful tool for the glycosylation analysis of serum proteins. For the glycosylation analysis of serum glycoproteins, the enrichment of glycopeptides by lectin-affinity or hydrophilic chromatography is useful due to their low ionization efficiency, ionization suppression effects, and microheterogeneity [16–19]. There are still concerns about the loss of some glycopeptides during the preparation procedure, biased recoveries toward certain glycan structures, and low reproducibility of recovery. Liquid chromatography/mass spectrometry (LC/MS) is effective for the separation of glycopeptides and for the simultaneous glycosylation analysis.

Abbreviations: ESI, electrospray ionization; Fuc, fucose; GlcNAc, N-acetylglucosamine; Hex, hexose; HexNAc, N-acetylhexosamine; HPLC, high-performance liquid chromatography; IgG, immunoglobulin G; MS, mass spectrometry; MS/MS, tandem mass spectrometry; NeuAc, N-acetylneuraminic acid; Qq-TOF, quadrupole–quadrupole time-of-flight mass spectrometry; TIC, total ion chromatogram; EIC, extracted ion chromatogram.

* Corresponding author. Tel.: +81 3 3700 9074; fax: +81 3 3700 9084.
E-mail addresses: harazono@nihs.go.jp (A. Harazono), nana@nihs.go.jp (N. Kawasaki).

1570-0232/$ – see front matter © 2008 Elsevier B.V. All rights reserved.
doi:10.1016/j.jchromb.2008.05.006

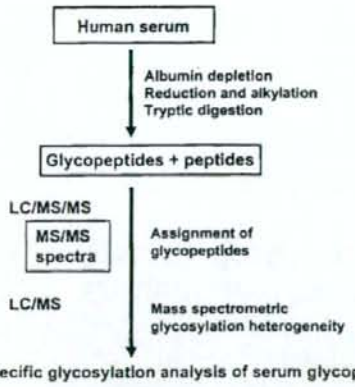

Fig. 1. Strategy for glycosylation analysis of abundant glycoproteins in serum. Human serum in which albumin was roughly removed was reduced and alkylated at cysteine residues. A mixture of peptides resulting from trypsin digestion was subjected to LC/MS/MS and LC/MS. Glycopeptides were assigned by elucidating MS/MS spectra (database searching). Mass spectrometric heterogeneity at each glycosylation site was analyzed by an additional LC/MS.

Recent progress in MS/MS and multiple-stage MS (MS^n) of glycopeptides allows for the characterization of both peptide and oligosaccharide moieties based on fragment ions [17,20–27]. Previously it was demonstrated that the Qq-TOF type mass spectrometer provides highly abundant carbohydrate-related ions at lower *m/z* values such as *m/z* 204 $[HexNAc+H]^+$ and 366 $[HexHexNAc+H]^+$, glycopeptide-related ions with sequentially lost saccharide units, including $[peptide+H]^+$ and $[peptide+GlcNAc+H]^+$ at higher *m/z* values, and *b*- and *y*-ions derived from peptide backbone [20,23,26,28]. These fragment ions could be used in database search to deduce peptide of glycopeptide.

In this study we demonstrated LC/MS(/MS) of human serum digest for the simultaneous glycosylation analysis of abundant serum proteins. Fig. 1 shows the strategy for the glycosylation analysis. Human serum, the albumin of which was depleted, was carboxymethylated and digested with trypsin. LC/MS/MS of the digest was performed by using the LC/Qq-TOF MS instrument. Glycopeptide ions were basically assigned by database searching with modified peak-list text files. Mass spectrometric heterogeneity at each glycosylation site was analyzed by an additional LC/MS, in which the acquisition of MS/MS was not allowed. By LC/MS of albumin-depleted human serum digest, we were successful in the site-specific glycosylation analysis of abundant serum glycoproteins.

2. Experimental

2.1. Materials

Pooled normal human serum was purchased from Sigma (St. Louis, MO, USA). Human haptoglobin and polyclonal immunoglobulin G, which were purified from normal human serum, were purchased from Calbiochem (San Diego, CA, USA). Modified trypsin was purchased from Promega (Madison, WI, USA). The water used was obtained from a Milli-Q water system (Millipore, Bedford, MA). All other reagents were of the highest quality available.

2.2. Sample preparation

Human serum (5 μl) was depleted of albumin using the Montage Albumin Depletion Kit (Millipore, Bedford, MA, USA) according to the manufacturer's protocol. Lyophilized albumin-depleted sample and each of the glycoproteins (100 μg) were dissolved in 50 μl of 0.5 M Tris–HCl buffer (pH 8.5) that contained 7 M guanidine hydrochloride and 5 mM EDTA. After the addition of 2 μl of 1 M dithiothreitol, the mixture was incubated for 30 min at 56 °C. Then, 4.7 μl of 1 M sodium monoiodoacetate was added, and the resulting mixture was incubated for 30 min at room temperature in the dark. The reaction mixture was applied to a PD-10 column (GE Healthcare, Little Chalfont, UK) to remove the reagents, and a fraction of the carboxymethylated proteins was dried. The sample was redissolved in 50 μl of 50 mM Tris–HCl buffer (pH 8.0). An aliquot of 1 μl of modified trypsin prepared as 1 μg/μl was added, and then the mixtures were incubated for 12 h at 37 °C. The enzyme digestions were stopped by boiling for 10 min and stored at −20 °C before analysis.

2.3. LC/MS and LC/MS/MS

The tryptic digests corresponding to 0.01–0.3 μl of human serum or a tryptic digest of purified commercially available glycoprotein (0.1–1.0 μg) was loaded onto a nanotrap (AMR Inc., Tokyo, Japan). After a wash with 10 μl of 2% (v/v) acetonitrile containing 0.1% (v/v) TFA, the trapping column was switched into line with the column. HPLC was performed on a Paradigm MS 4 (Michrome BioResources, Auburn, CA, USA) equipped with a MonoCap High Resolution 750 column (0.2 mm × 750 mm, GL Sciences Inc., Tokyo, Japan) at a flow rate of about 2 μl/min. The eluents consisted of water containing 2% (v/v) acetonitrile and 0.1% (v/v) formic acid (pump A) and 90% acetonitrile and 0.1% formic acid (pump B). Samples were eluted with 5% of B for 2.5 or 5.0 min followed by a linear gradient from 5 to 90% of pump B in 85 min or by linear gradients from 5 to 25% for 80 min, 25–45% for the next 60 min, 45–65% for the next 40 min and 60–90% for the next 20 min (total 205 min).

Mass spectrometric analyses were performed using a QSTAR Pulsar i Qq-TOF mass spectrometer (AB/MDS Sciex, Toronto, Canada) equipped with a nano-electrospray ion source. The mass spectrometer was operated in positive ion mode. The nano-spray voltage was set at 1700 V. Mass spectra were acquired over *m/z* 1000–2000 for MS, and *m/z* 100–2000 for MS/MS. After every regular MS acquisition, MS/MS acquisitions were performed against the top two multiply charged ions by a data-dependent acquiring method. The precursor ions with the same *m/z* as previously acquired were excluded for 60 or 90 s. The collision energy was varied between 30 and 70 eV depending on the size and charge of the molecular ion. The accumulation time of the spectra was 1.0 s for MS, and 2.0 or 5.0 s for MS/MS. All signals were monoisotopically resolved.

2.4. Assignment of glycopeptide peaks by database search

Detection and assignment of glycopeptide ions from LC/ESI MS/MS data were performed by elucidating MS/MS spectra or database search. Briefly, glycopeptide ions were selected manually based on presence of oligosaccharide oxonium ions such as *m/z* 204 and 366 in their MS/MS spectra. The information of *m/z* values and charge states of peptides in the glycopeptides was deduced by sequential degradation pattern at N-glycan core structure in their MS/MS spectra. The MS/MS spectra of glycopeptides were converted to peak-list text files, and then oligosaccharide-related ions (*m/z* 168, 186, 204, 274, 292 and 366 or ions under *m/z* 370)

and the ions larger than peptide ion were deleted. Modified peak-list text files were submitted to against the nonredundant human Swiss–Prot protein database (version 48.2) using Mascot search engine with following parameters: a specified trypsin enzymatic cleavage with two possible missed cleavage, peptide tolerance of 1.2 Da, fragment ion tolerance of 0.8 Da, and variable modifications of cysteine (carboxymethylation) or cystein (carboxymethylation) and methionine (oxidation). Suggested peptides were validated by manual inspection of the spectra, and the presence of more than four consecutive fragments of amino acid sequence was used as criteria for peptide identification.

3. Results

3.1. Locating glycopeptides in the chromatogram

Mass spectrometric glycosylation analysis of human serum was performed by LC/Qq-TOF MS of tryptic digest using in a positive ion mode. In this method, all serum glycoproteins should be completely digested by trypsin. When the tryptic digest was subject to LC/MS/MS with the MS range m/z 400–2000, results of Mascot database search using 3 missed cleavage sites suggested that most peptides were completely digested (missed cleavage <1) and few incompletely digested peptides (missed cleavage 3) were present. Many missed cleavage sites were present at N- or C-terminal, or adjacent to two or more acidic amino acid residues (D, E or carboxymethylated C) (data not shown). Fig. 2A shows the total ion chromatogram (TIC) obtained by LC/MS/MS with MS range m/z 1000–2000 of tryptic digest (corresponding to approximately 0.3 μl of serum) using a reversed phase MonoCap High Resolution 750 column (0.2 mm × 750 mm) with a gradient of 5–90% of B in 205 min. In order to locate the glycopeptide peaks and determine m/z and charge state, the intensity of the oxonium HexNAc$^+$ (m/z 204.05–204.15) that arose by data-dependent MS/MS was depicted as the extracted ion chromatogram (Fig. 2B). We confirmed that most of these MS/MS spectra were of glycopeptides by the presence of abundant carbohydrate-derived ions, such as m/z 204 ([HexNAc+H]$^+$), 186 ([HexNAc+H−H_2O]$^+$), 292 ([NeuAc+H]$^+$), 274 ([NeuAc+H−H_2O]$^+$) and 366 ([HexHexNAc+H]$^+$).

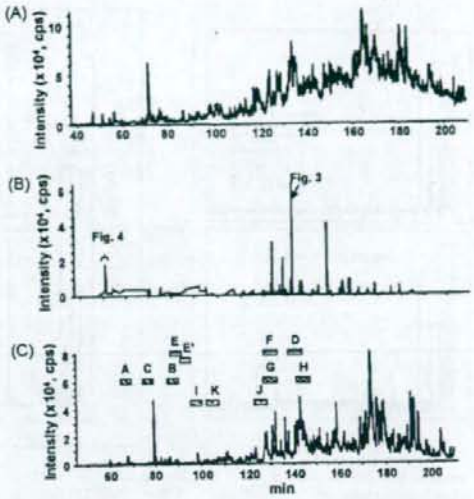

Fig. 2. LC/MS/MS and LC/MS of tryptic digest of human serum. (A) TIC (m/z 1000–2000) obtained by the LC/MS/MS. (B) EIC (m/z 204.05–204.15) obtained by the data-dependent MS/MS. (C) TIC obtained by the additional LC/MS in which data-dependent MS/MS was not allowed. Peak assignment: A, IgG1; B, IgG2; C, IgG3/IgG4; D–F, haptoglobin; G and H, transferrin; I–K, ceruloplasmin. Mass spectra of fractions A–K are shown in Fig. 7.

3.2. Assignment of glycopeptide peaks by a database search

Glycopeptides were assigned by manual database searching. As a representative example, the MS/MS spectrum acquired from [M+4H]$^{4+}$ (m/z 1221.8 (4+)) at 133 min is shown in Fig. 3. There are some abundant ions derived from carbohydrates, such as m/z 204, 186, 292, 274 and 366 in the lower m/z region. Degradation pattern and mass difference of 203 u between the fragment ions at m/z 1340.2 (2+) and those at 1441.7 (2+) in the higher m/z region suggests that the ions are [peptide+2H]$^{2+}$ and [peptide+HexNAc+2H]$^{2+}$, respectively. Based on these m/z values the molecular mass of

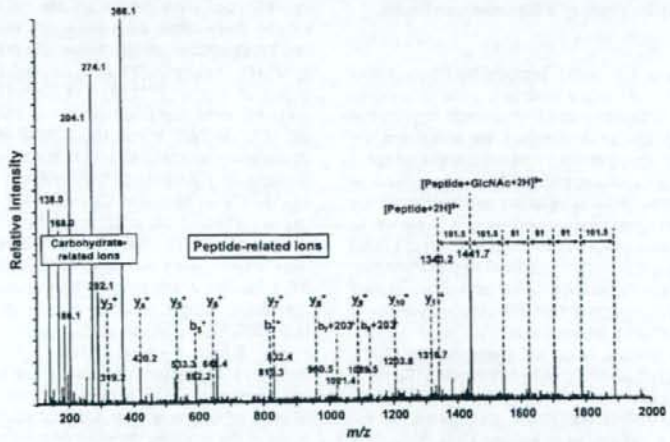

Fig. 3. MS/MS spectrum acquired from m/z 1221.8 (4+) by data-dependent LC/MS/MS of trypsin-digested human serum. Mascot database search using m/z 1340.2 (2+) of peptide and fragment ions (m/z 370–1300) suggested peptide sequence MVSHHN^{184}LTTGATLINEQWLLTTAK in haptoglobin (P00738).

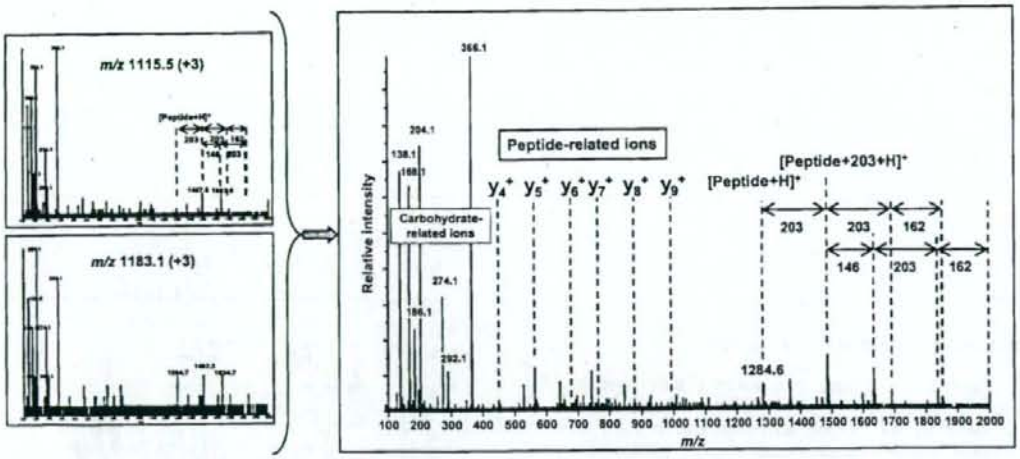

Fig. 4. Integrated MS/MS spectrum of *m/z* 1115.5 (3+) and 1183.1 (3+) at 52–53 min that show similar fragment patterns. Mascot database search using *m/z* 1284.5 (1+) of peptide and fragment ions (*m/z* 370–1280) suggested YKN[46]NSDISSTR in Ig mu chain C region (P01871).

the peptide was calculated to be 2678.4. For the peptide identification, a database search requires the *m/z* values and charge state of the peptide precursor ions and fragment ions but not of the carbohydrate- and glycopeptide-related ions. We deleted the carbohydrate-related ions in the lower *m/z* region (under *m/z* 370) and the glycopeptide-related ions in the higher *m/z* region (over *m/z* 1340) from the peak-list text files, and then submitted the modified peak-list text files for a Mascot database search of the human Swiss–Prot database with 1 missed cleavage, peptide tolerance of 1.2 Da, fragment ion tolerance of 0.8 Da and variable modifications of cysteine (carboxymethylation). The peptide suggested was MVSHHN[184]LTTGATLINEQWLLTTAK in human haptoglobin (P00738). As shown in Fig. 3, many ions were consistent with *b*- and *y*-series peptide fragment ions derived form MVSHHNLTTGATLINEQWLLTTAK. The molecular mass of the carbohydrate moiety was calculated to be 2204.7, which suggests the carbohydrate composition of $HexNAc_4Hex_5NeuAc_2$.

3.3. Assignment of glycopeptide peaks by a database search with integrated spectra

Glycopeptides that have the same peptide backbone show quite similar fragment patterns in the case of Qq-TOF MS. When glycopeptides showed insufficient peptide fragment ions in the CID-MS/MS spectra due to low peak intensity, we integrated the similar MS/MS spectra into one spectrum, and the integrated spectrum was submitted for a database search. As a representative example, the spectrum obtained by integrating two spectra of *m/z* 1115.5 (3+) and 1183.1 (3+) acquired around 60 min is shown in Fig. 4. Mascot database search using the information of *m/z* 1284.5 (1+) of peptide which was deduced by sequential degradation pattern at N-glycan core structure, and modified peak-list text files between *m/z* 370 and 1250 suggests that the peptide moiety is YKN[46]NSDISSTR in Ig mu chain C region (P01871).

By elucidating MS/MS spectra, 19 tryptic glycopeptides (20 N-glycosylation sites) in 14 glycoproteins were determined (Table 1). The ions, which were confirmed as glycopeptides by data-dependent MS/MS, were underlined. Other glycoforms, whose MS/MS spectra were not acquired, were assigned based on their mass difference of saccharide units from characterized glycopeptides. Since high intensity glycopeptide ions showed high quality of MS/MS spectra and were subjected to data-dependent MS/MS several times, many of them could be assigned. Low intensity glycopeptide ions showed poor MS/MS spectra for detection of peptide fragment ions, about 20% of MS/MS spectra of glycopeptides could not be assigned (data not shown).

3.4. Confirmation of glycopeptide peaks using commercially available glycoproteins

We conducted peptide mapping of commercially available polyclonal IgG and haptoglobin, and then *m/z* values and charge states of the glycopeptides were used for confirmation of assignment of glycopeptides and assignment of undetected glycopeptides. Glycosylation data of ceruloplasmin in previous report [28] was also utilized.

Tryptic digest (0.2 μg and 0.4 μg) of commercially available human polyclonal IgG was analyzed by LC/ESI MS/MS at *m/z* 400–2000 and 1000–2000 with a gradient of 5–90% of B in 85 min. The MS data were submitted for database searching against the human Swiss–Prot database using the computer program Mascot. Polypeptides of IgG heavy chain C region of IgG1 (P01857), IgG2 (P01859), IgG3 (P01860) and IgG4 (P01861) and light chain C region of Kappa (P01834) and Lambda (P01842) chain and other proteins were identified (data not shown). Fig. 5A and A′ show TIC of LC/MS/MS at *m/z* 1000–2000 of polyclonal IgG and EIC of data-dependent MS/MS at *m/z* 204.05–205.15, respectively. It was found that glycopeptide ions were eluted at 7–12 min (fraction A), 15–17 min (fraction C) and 18–21 min (fraction B) based on the presence of the oligosaccharide-related ions in their MS/MS spectra and mass differences of saccharide units. MS/MS spectra after 25 min were not of glycopeptides. The glycopeptide peaks from fraction A and fraction B were assigned as the glycopeptides containing Fc-glycosylation site in IgG1 (EEQYNSTYR) and IgG2 (EEQFNSTFR) based on data-dependent MS/MS spectra, respectively (data not shown). Data-dependent MS/MS spectra from fraction C suggested molecular mass of 1171.5 Da for the peptide, but could not suggest amino acid sequence due to low abundance of peptide fragment ions (data not shown). Based on the molecular mass of the peptide, the glycopeptide peaks from fraction C would be EEQYNSTFR from IgG3 (CAA67886) and/or EEQFNSTYR from IgG4 (P01861), which are attached to core-fucosylated agalacto-

Table 1
Summary of analysis of serum glycoproteome with higher ion intensities

Glycopeptide					Oligosaccharide	Protein (Protein ID)	Theoretical MW
Retention time (min)	m/z[a]	Charge	Observed MW	Relative peak intensity[b]	Observed MW	Glycopeptide Peptide sequence Deduced oligosaccharide composition[c]	Peptide Oligosaccharide
						Ig gamma-1 chain C region (P01857)	1[d]
						EEQYNSTYR[A]	1188.50
67.3	1479.6	2+	2957.1	13.1	1768.6	[HexNAc]4[Hex]5[Fuc]1	1768.64
67.3	1297.0	2+	2592.0	3.0	1403.5	[HexNAc]3[Hex]4[Fuc]1	1403.51
67.4, 67.6	1398.5	2+	2795.1	33.1	1606.5	[HexNAc]4[Hex]4[Fuc]1	1606.59
67.4, 67.7	1216.0	2+	2429.9	4.3	1241.4	[HexNAc]3[Hex]3[Fuc]1	1241.45
67.7	1317.5	2+	2633.0	27.8	1444.5	[HexNAc]4[Hex]3[Fuc]1	1444.53
67.9	1500.1	2+	2998.1	2.3	1809.6	[HexNAc]5[Hex]4[Fuc]1	1809.67
	1000.4	3+	2998.0				
67.9	1581.1	2+	3160.2	0.2	1971.7	[HexNAc]5[Hex]5[Fuc]1	1971.72
68.0	1406.6	2+	2811.1	0.9	1622.6	[HexNAc]4[Hex]5	1622.58
68.2, 68.4	1325.5	2+	2649.0	2.8	1460.5	[HexNAc]4[Hex]4	1460.53
68.2	1419.1	2+	2836.1	2.9	1647.6	[HexNAc]5[Hex]3[Fuc]1	1647.61
68.5	1244.5	2+	2486.9	1.4	1298.4	[HexNAc]4[Hex]3	1298.48
69.1	1625.1	2+	3248.1	2.2	2059.6	[HexNAc]4[Hex]5[NeuAc]1[Fuc]1	2059.73
	1083.7	3+	3248.1				
69.6	1544.1	2+	3086.2	0.5	1897.6	[HexNAc]4[Hex]4[NeuAc]1[Fuc]1	1897.68
						EEQYNSTYRVVSVLTVLHQDWLNGK[B]	2977.49
161.9, 162.2	1147.0	4+	4584.1		1606.6	[HexNAc]4[Hex]4[Fuc]1	1606.59
162.4	1106.5	4+	4422.1		1444.6	[HexNAc]4[Hex]3[Fuc]1	1444.53
						EEQYNSTYRVVSVLTVLHQDWLNGKEYK[B]	3397.69
156.4	1034.3	5+	5166.4		1768.7	[HexNAc]4[Hex]5[Fuc]1	1768.64
156.6, 157.1	1001.8	5+	5004.0		1606.3	[HexNAc]4[Hex]4[Fuc]1	1606.59
						Ig gamma-2 chain C region (P01859)	1[d]
						EEQFNSTFR[B]	1156.51
85.4	1463.6	2+	2925.1	6.3	1768.6	[HexNAc]4[Hex]5[Fuc]1	1768.64
85.5	1281.0	2+	2560.0	1.4	1403.5	[HexNAc]3[Hex]4[Fuc]1	1403.51
85.7, 86.3	1382.5	2+	2763.1	19.4	1606.5	[HexNAc]4[Hex]4[Fuc]1	1606.59
85.7, 86.4	1200.0	2+	2397.9	2.8	1241.4	[HexNAc]3[Hex]3[Fuc]1	1241.45
85.7	1565.1	2+	3128.2	0.0	1971.7	[HexNAc]5[Hex]5[Fuc]1	1971.72
86.0	1484.1	2+	2966.2	1.0	1809.6	[HexNAc]5[Hex]4[Fuc]1	1809.67
86.5	1301.5	2+	2601.0	21.8	1444.5	[HexNAc]4[Hex]3[Fuc]1	1444.53
86.5	1390.5	2+	2779.0	0.0	1622.5	[HexNAc]4[Hex]5	1622.58
86.9	1403.0	2+	2804.1	1.8	1647.5	[HexNAc]5[Hex]3[Fuc]1	1647.61
87.0, 87.5	1309.5	2+	2617.0	0.1	1460.5	[HexNAc]4[Hex]4	1460.53
87.6	1228.5	2+	2454.9	0.2	1298.4	[HexNAc]4[Hex]3	1298.48
89.4	1609.1	2+	3216.2	1.6	2059.7	[HexNAc]4[Hex]5[NeuAc]1[Fuc]1	2059.73
	1073.1	3+	3216.2				
90.0	1528.1	2+	3054.2	1.5	1897.6	[HexNAc]4[Hex]4[NeuAc]1[Fuc]1	1897.68
	1019.1	3+	3054.1				
						Gamma 3 immunoglobulin constant heavy chain (CAA67886)	2[d]
						EEQYNSTFR[C]	1172.51
						Ig gamma-4 chain C region (P01861)	1[d]
						EEQFNSTYR[C]	1172.51
76.4	1471.6	2+	2941.1	1.0	1768.6	[HexNAc]4[Hex]5[Fuc]1	1768.64
76.5	1289.0	2+	2576.0	0.2	1403.5	[HexNAc]3[Hex]4[Fuc]1	1403.51
76.6, 76.8	1390.6	2+	2779.1	3.4	1606.6	[HexNAc]4[Hex]4[Fuc]1	1606.59
76.5, 76.8	1208.0	2+	2413.9	0.4	1241.4	[HexNAc]3[Hex]3[Fuc]1	1241.45
76.7	1492.1	2+	2982.1	0.2	1809.6	[HexNAc]5[Hex]4[Fuc]1	1809.67
76.9	1309.5	2+	2617.0	3.6	1444.5	[HexNAc]4[Hex]3[Fuc]1	1444.53
77.0	1398.6	2+	2795.1	0.1	1622.6	[HexNAc]4[Hex]5	1622.58
76.9	1317.5	2+	2633.0	0.1	1460.5	[HexNAc]4[Hex]4	1460.53
77.0	1411.1	2+	2820.1	0.3	1647.6	[HexNAc]5[Hex]3[Fuc]1	1647.61
77.4	1236.4	2+	2470.8	0.1	1298.3	[HexNAc]4[Hex]3	1298.48
78.5	1617.1	2+	3232.1	0.3	2059.6	[HexNAc]4[Hex]5[NeuAc]1[Fuc]1	2059.73
79.1	1536.1	2+	3070.1	0.1	1897.6	[HexNAc]4[Hex]4[NeuAc]1[Fuc]1	1897.68
						Haptoglobin (P00738)	4[d]
						MVSHHNLTTGATLINEQWLLTTAK[C]	2678.39
137.9	1531.7	3+	4592.1		1913.7	[HexNAc]4[Hex]5[NeuAc]1	1913.68
	1149.0	4+	4592.0	30.1	1913.6		

Table 1 (*Continued*)

Glycopeptide					Oligosaccharide	Protein (Protein ID)	Theoretical MW
Retention time (min)	m/z[a]	Charge	Observed MW	Relative peak intensity[b]	Observed MW	Glycopeptide	Peptide
						Peptide sequence Deduced oligosaccharide composition[c]	Oligosaccharide
141.4	1221.8	4+	4883.1	88.7	2204.7	[HexNAc]4[Hex]5[NeuAc]2	2204.77
137.3	1153.0	4+	4608.1	28.9	1913.7	M(O)VSHHNLTTGATLINEQWLLTTAK [HexNAc]4[Hex]5[NeuAc]1	2694.38 1913.68
140.5, 141.1	1225.8	4+	4899.1	64.3	2204.7	[HexNAc]4[Hex]5[NeuAc]2	2204.77
	1634.1	3+	4899.1		2204.8		
86.3	1395.0	4+	5576.0	0.1	4118.3	NLFLNHSENATAK[E]	1457.73
87.0	1650.3	4+	6597.3	0.3	5139.6	[HexNAc]8[Hex]10[NeuAc]3	4118.45
87.6	1595.6	4+	6378.3	0.9	4920.6	[HexNAc]10[Hex]12[NeuAc]4	5139.81
87.9	1559.1	4+	6232.3	2.7	4774.5	[HexNAc]9[Hex]11[NeuAc]4[Fuc]1	4920.73
88.6	1504.3	4+	6013.0	0.1	4555.3	[HexNAc]9[Hex]11[NeuAc]4	4774.68
88.9	1467.8	4+	5867.1	4.1	4409.4	[HexNAc]8[Hex]10[NeuAc]4[Fuc]1	4555.60
90.4	1759.6	4+	7034.5	0.2	5576.8	[HexNAc]8[Hex]10[NeuAc]4	4409.54
90.7	1723.1	4+	6888.5	0.5	5430.8	[HexNAc]10[Hex]12[NeuAc]5[Fuc]1	5576.96
91.5	1668.3	4+	6669.4	0.3	5211.6	[HexNAc]10[Hex]12[NeuAc]5	5430.90
91.7	1631.8	4+	6523.3	0.4	5065.6	[HexNAc]9[Hex]11[NeuAc]5[Fuc]1	5211.83
87.8	1124.7	3+	3371.2	-	1913.5	[HexNAc]9[Hex]11[NeuAc]5	5065.77
91.6	1221.7	3+	3662.2	-	2204.5	[HexNAc]4[Hex]5[NeuAc]1	1913.68
						[HexNAc]4[Hex]5[NeuAc]2	2204.77
127	1358.6	3+	4072.8	2.2	2278.8	VVLHPNYSQVDIGLIK[F]	1794.00
128.2	1236.9	3+	3707.7	3.1	1913.7	[HexNAc]5[Hex]6[NeuAc]1	2278.81
131.4	1455.6	3+	4363.8	4.8	2569.8	[HexNAc]4[Hex]5[NeuAc]1	1913.68
	1092.0	4+	4363.8			[HexNAc]5[Hex]6[NeuAc]2	2569.90
131.8	1333.9	3+	3998.7	89.2	2204.7	[HexNAc]4[Hex]5[NeuAc]2	2204.77
	1000.7	4+	3998.7		2204.7		
134.1	1552.7	3+	4655.0	7.5	2860.9	[HexNAc]5[Hex]6[NeuAc]3	2861.00
134.1	1164.7	4+	4654.9		2860.9		
						Transferrin (P02787)	2[d]
126.1	1252.8	3+	3755.5	0.9	2278.8	CGLVPVLAENYNK[G]	1476.73
127.0	1131.1	3+	3390.4	1.7	1913.7	[HexNAc]5[Hex]6[NeuAc]1	2278.81
129.8	1349.9	3+	4046.7	1.6	2569.9	[HexNAc]4[Hex]5[NeuAc]1	1913.68
130.6	1228.2	3+	3681.5	46.8	2204.7	[HexNAc]5[Hex]6[NeuAc]2	2569.90
133.1	1446.9	3+	4337.8	0.8	2861.0	[HexNAc]4[Hex]5[NeuAc]2	2204.77
						[HexNAc]5[Hex]6[NeuAc]3	2861.00
143.8	1623.3	3+	4866.9	4.1	2350.8	QQQHLFGSNVTDCSGNFCLFR[H]	2516.08
143.9	1181.2	4+	4720.9		2204.8	[HexNAc]4[Hex]5[NeuAc]2[Fuc]1	2350.83
	1574.6	3+	4720.9	50.5	2204.8	[HexNAc]4[Hex]5[NeuAc]2	2204.77
146.0	1842.0	3+	5523.0	0.9	3007.0	[HexNAc]5[Hex]6[NeuAc]3[Fuc]1	3007.06
146.2	1793.4	3+	5377.3	1.6	2861.2	[HexNAc]5[Hex]6[NeuAc]3	2861.00
						Ceruloplasmin (P00450)	4[d]
95.6	1415.2	3+	4242.7	0.1	2350.8	EHEGAIYPDNTTDFQR[I]	1891.83
	1061.7	4+	4242.6		2350.8	[HexNAc]4[Hex]5[NeuAc]2[Fuc]1	2350.83
96.3	1366.5	3+	4096.6	6.0	2204.8	[HexNAc]4[Hex]5[NeuAc]2	2204.77
	1025.2	4+	4096.7		2204.9		
98.1, 98.5	1633.9	3+	4898.7	0.4	3006.9	[HexNAc]5[Hex]6[NeuAc]3[Fuc]1	3007.06
	1226.0	4+	4899.9		3008.0		
98.8	1585.2	3+	4752.7	0.4	2860.9	[HexNAc]5[Hex]6[NeuAc]3	2861.00
	1189.2	4+	4752.6		2860.8		
127.0	1493.2	3+	4476.6	0.0	2350.6	ENLTAPGSDSAVFFEQGTTR[J]	2125.99
127.4	1444.5	3+	4330.6	2.8	2204.6	[HexNAc]4[Hex]5[NeuAc]2[Fuc]1	2350.83
129.3	1663.3	3+	4987.0	0.2	2861.0	[HexNAc]4[Hex]5[NeuAc]2	2204.77
						[HexNAc]5[Hex]6[NeuAc]3	2861.00
104.3	1093.9	4+	4371.7	1.4	2350.7	ELHHLQEQNVSNAFLDK[K]	2021.00
	1458.3	3+	4371.8	0.2	2350.8	[HexNAc]4[Hex]5[NeuAc]2[Fuc]1	2350.83
105.2	1057.4	4+	4225.7	4.5	2204.7	[HexNAc]4[Hex]5[NeuAc]2	2204.77
	1409.6	3+	4225.6	1.2	2204.6		

Table 1 (*Continued*)

Glycopeptide					Oligosaccharide	Protein (Protein ID)	Theoretical MW
Retention time (min)	m/z[a]	Charge	Observed MW	Relative peak intensity[b]	Observed MW	Glycopeptide Peptide sequence Deduced oligosaccharide composition[c]	Peptide Oligosaccharide
106.6	1294.6	4+	5174.2	1.2	3153.2	[HexNAc]5[Hex]6[NeuAc]3[Fuc]2	3153.12
106.8, 107.4	1258.0	4+	5027.9	2.0	3006.9	[HexNAc]5[Hex]6[NeuAc]3[Fuc]1	3007.06
107.7	1221.5	4+	4881.8	1.9	2860.8	[HexNAc]5[Hex]6[NeuAc]3	2861.00
						Alpha-1-antitrypsin (P01009)	3[d]
						YLGNATAIFFLPDEGK	1754.89
154.6	1369.6	3+	4105.7	2.2	2350.8	[HexNAc]4[Hex]5[NeuAc]2[Fuc]1	2350.83
154.8	1320.9	3+	3959.7	140.6	2204.8	[HexNAc]4[Hex]5[NeuAc]2	2204.77
						Alpha-2-HS-glycoprotein (P02765)	2[d]
						VCQDCPLLAPLNDTR	1772.81
136.9	1326.9	3+	3977.7		2204.8	[HexNAc]4[Hex]5[NeuAc]2	2204.77
						Alpha-2-macroglobulin (P01023)	8[d]
						VSNQTLSLFFTVLQDVPVR	2162.17
187.9, 188.8	1505.3	3+	4512.7	5.1	2350.6	[HexNAc]4[Hex]5[NeuAc]2[Fuc]1	2350.83
188.3	1456.7	3+	4367.0	22.5	2204.8	[HexNAc]4[Hex]5[NeuAc]2	2204.77
						Beta-2-glycoprotein 1 (P02749)	4[d]
						VYKPSAGNNSLYR	1467.75
83.5	1273.8	3+	3818.5	1.5	2350.8	[HexNAc]4[Hex]5[NeuAc]2[Fuc]1	2350.83
83.6	1225.2	3+	3672.5	6.9	2204.8	[HexNAc]4[Hex]5[NeuAc]2	2204.77
85.2	1492.6	3+	4474.6	0.3	3006.9	[HexNAc]5[Hex]6[NeuAc]3[Fuc]1	3007.06
85.4	1443.9	3+	4328.6	0.5	2860.8	[HexNAc]5[Hex]6[NeuAc]3	2861.00
						LGNWSAMPSCK	1250.54
109.7	1152.8	3+	3455.3		2204.7	[HexNAc]4[Hex]5[NeuAc]2	2204.77
						Complement C3 (P01024)	3[d]
						TVLTPATNHMGNVTFTIPANR	2254.15
121.0	1265.9	3+	3794.6	5.4	1540.4	[HexNAc]2[Hex]7	1540.53
121.2	1211.8	3+	3632.5	47.8	1378.4	[HexNAc]2[Hex]6	1378.48
121.6	1157.8	3+	3470.4	10.2	1216.3	[HexNAc]2[Hex]5	1216.42
						Hemopexin (P02790)	5[d]
						SWPAVGNCSSALR	1404.65
115.3	1252.8	3+	3755.5	0.7	2350.8	[HexNAc]4[Hex]5[NeuAc]2[Fuc]1	2350.83
115.8	1204.1	3+	3609.4	10.3	2204.7	[HexNAc]4[Hex]5[NeuAc]2	2204.77
						ALPQPQNVTSLLGCTH	1735.86
115.8	1314.5	3+	3940.4	10.3	2204.5	[HexNAc]4[Hex]5[NeuAc]2	2204.77
						Ig alpha-1 chain C region (P01876)	2[d]
						Ig alpha-2 chain C region (P01877)	4[d]
						LSLHRPALEDLLLGSEANLTCTLTGLR	2963.58
165.2, 165.7	1157.8	4+	4627.2	8.0	1663.6	[HexNAc]5[Hex]4	1663.61
165.8	1117.3	4+	4465.0	15.4	1501.4	[HexNAc]5[Hex]3	1501.56
165.9	1046.0	4+	4180.0	5.6	1216.4	[HexNAc]2[Hex]5	1216.42
169.2	1220.3	4+	4877.2	48.8	1913.6	[HexNAc]4[Hex]5[NeuAc]1	1913.68
168.8, 169.4	1256.9	4+	5023.5	1.3	2059.9	[HexNAc]4[Hex]5[NeuAc]1[Fuc]1	2059.73
169.9	1179.8	4+	4715.3	4.0	1751.7	[HexNAc]4[Hex]4[NeuAc]1	1751.62
170.0	1169.6	4+	4674.2	5.1[f]	1710.6	[HexNAc]3[Hex]5[NeuAc]1	1710.60
169.0	1271.2	4+	5080.8	21.0[f]	2117.2	[HexNAc]5[Hex]5[NeuAc]1	2116.76
	1017.2	5+	5081.0		2117.4		
169.9	1230.4	4+	4917.6	11.8	1954.0	[HexNAc]5[Hex]4[NeuAc]1	1954.70
173.1	1293.2	4+	5168.8	9.0	2205.2	[HexNAc]4[Hex]5[NeuAc]2	2204.77
						PALEDLLLGSEANLTCTLTGLR[e]	2357.21
174.4	1287.2	3+	3858.6	14.3	1501.4	[HexNAc]5[Hex]3	1501.56
176.7	1424.6	3+	4270.9	65.8	1913.7	[HexNAc]4[Hex]5[NeuAc]1	1913.68
176.4	1492.5	3+	4474.5	20.5	2117.3	[HexNAc]5[Hex]5[NeuAc]1	2116.76
						Ig alpha-2 chain C region (P01877)	
						TPLTANITK	957.55
84.1	1006.8	3+	3017.2	3.7	2059.7	[HexNAc]4[Hex]5[NeuAc]1[Fuc]1	2059.73
	1509.6	2+	3017.2		2059.6		
84.1	1074.4	3+	3220.3	4.8	2262.8	[HexNAc]5[Hex]5[NeuAc]1[Fuc]1	2262.81
	1611.2	2+	3220.3		2262.8		
87.2	1103.8	3+	3308.3	1.3	2350.8	[HexNAc]4[Hex]5[NeuAc]2[Fuc]1	2350.83
						Ig mu chain C region (P01871)	5[d]
						YKNNSDISSTR[e]	1283.61

Table 1 (*Continued*)

Glycopeptide					Oligosaccharide	Protein (Protein ID)	Theoretical MW
Retention time (min)	m/z[a]	Charge	Observed MW	Relative peak Intensity[b]	Observed MW	Glycopeptide Peptide sequence Deduced oligosaccharide composition[c]	Peptide Oligosaccharide
59.7	1115.5	3+	3343.4	40.1	2059.7	[HexNAc]4[Hex]5[NeuAc]1[Fuc]1	2059.73
60.3	1183.1	3+	3546.4	16.4	2262.8	[HexNAc]5[Hex]5[NeuAc]1[Fuc]1	2262.81

[a] Underlines indicated that these ions were assigned by elucidating data-dependent MS/MS of LC/ESI MS/MS of human serum digest.
[b] Centroid peak intensity (count per sec) in integrated MS spectra during glycopeptide eluting period.
[c] Oligosaccharide compositions were deduced from molecular weights.
[d] Number of potential N-glycosylation sites.
[e] Missed cleavage or unexpected digestion.
[f] Other ions with same m/z overlapped.
[A–K] Mass spectra were shown in Fig. 7A–K.
All masses are monoisotopic. Cysteine residue was carboxymethylated. Potential N-glycosylation sites were underlined. M(O), oxidized methionine; Fuc, fucose; Hex, hexose; HexNAc, N-acetylhexosamine; NeuAc, N-acetylneuraminic acid

or mono/diagalacto-biantennary complex-type glycan. Integrated mass spectra of fraction A, B and C were shown in Fig. 5B–D.

Haptoglobin has four potential N-glycosylation sites. We performed peptide mapping using a tryptic digest of haptoglobin under a chromatographic condition similar to that of human serum. Fig. 6A and A′ show TIC obtained by LC/MS/MS with mass range m/z 1000–2000 and EIC of data-dependent MS/MS at m/z 204.05–205.15, respectively. Glycopeptides for four potential glycosylation sites were assigned by elucidating MS/MS spectra (spectra were not shown). Glycopeptides of NLFLN^{207}HSEN^{211}ATAK containing two N-glycosylation sites were eluted in fraction E as two glycosylated forms (Fig. 6B) and fraction E′ as one glycosylated forms (Fig. 6C). The former glycosylated form was more abundant than the later form. These glycosylation sites could not be characterized separately by trypsin digestion. Glycopeptides of VVLHPN^{241}YSQVDIGLIK and MVSHHN^{184}LTTGATLINEQWLLTTAK were eluted in fractions F and D, respectively (Fig. 6D and E). From the molecular masses of oligosaccharides we inferred that a majority of oligosaccharides in haptoglobin are di-, tri-, and tetra-antennary forms and that some oligosaccharides were not fully saturated with NeuAc, and few glycans were fucosylated.

Using the data of relative retention times, accurate m/z values and charge states obtained by peptide mapping of commercially available glycoproteins, we confirmed already assigned glycopeptides and further assigned undetected glycopeptides (IgG3/IgG4 and two sites of ceruloplasmin), with the exceptions of one of the glycopeptides from ceruloplasmin, intensity of which was only noise levels.

3.5. Site-specific glycosylation analysis

To analyze the heterogeneity of glycosylation at each site, we performed an additional LC/MS in which switching to MS/MS was not allowed (Fig. 2C). Utilizing the information of retention time, accurate m/z and charge state of assigned glycopeptides by LC/MS/MS, corresponding glycopeptides were assigned in LC/MS data by mass chromatogram. When two or more glycoforms were detected, mass spectrometric heterogeneity was calculated using

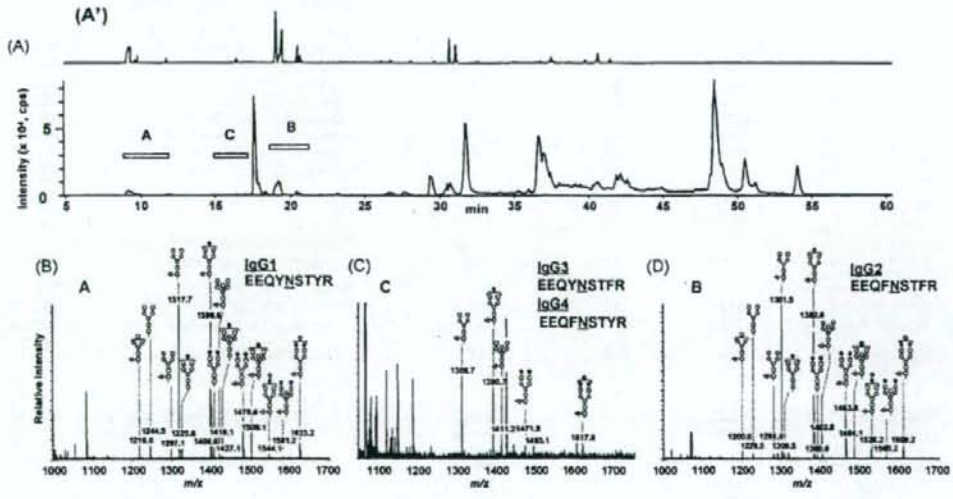

Fig. 5. Peptide map of commercially available human polyclonal IgG. (A) TIC (m/z 1000–2000) obtained by LC/MS/MS of trypsin-digested IgG. (A′) EIC (m/z 204.05–204.15) obtained by data-dependent MS/MS. (B) Mass spectrum of peak A, which was assigned as glycopeptides of EEQYNSTYR of IgG.1 (P01857). (C) Mass spectrum of peak C, which would be glycopeptides of EEQYNSTFR of IgG3 (CAA67886) and/or EEQFNSTYR of IgG4 (P01861). (D) Mass spectrum of peak B, which was assigned as glycopeptides of EEQFNSTFR of IgG2 (P01859).

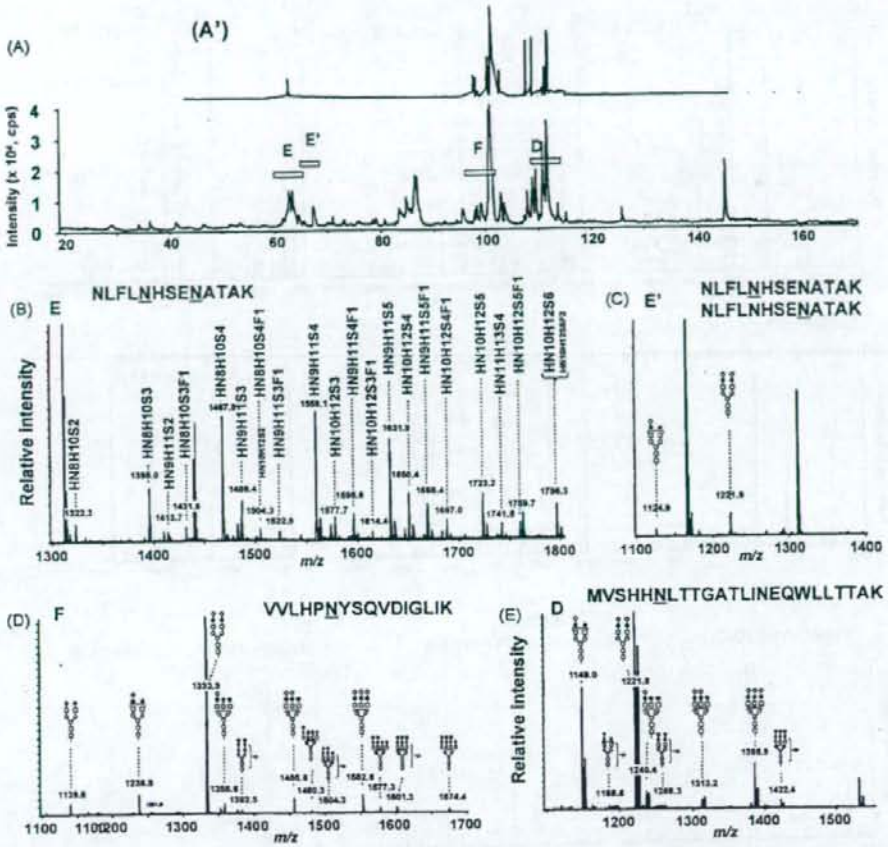

Fig. 6. Peptide map of commercially available human haptoglobin. (A) TIC (*m/z* 1000–2000) obtained by LC/MS/MS of trypsin-digested haptoglobin. (A') EIC (*m/z* 204.05–204.15) obtained by data-dependent MS/MS. (B) Mass spectrum of peak E, which was assigned as glycopeptides of NLFLN^{207}HSEN^{211}ATAK attached to two N-glycan. (C) Mass spectrum of peak E', which was assigned as glycopeptides of NLFLN^{207}HSEN^{211}ATAK attached to one N-glycan. (D) Mass spectrum of peak F, which was identified as VVLHPN^{241}YSQVDIGLIK. (E) Mass spectrum of peak D, which was identified as MVSHHN^{184}LTTGATLINEQWLLTTAK. H, hexose; HN, *N*-acetylhexosamine; S, *N*-acetylneuraminic acid; F, fucose.

integrated mass spectra during the periods eluting the glycopeptides with same peptide. In Fig. 7, we show integrated mass spectra of fraction A–K (Fig. 2C) as the mass spectrometric heterogeneity of glycosylation in IgG1 (Fig. 7A), IgG2 (Fig. 7B), IgG3/IgG4 (Fig. 7C), haptoglobin (Fig. 7D–F), transferrin (Fig. 7G and H) and ceruloplasmin (Fig. 7I–K). Centroid ion intensity (count/sec) of each glycopeptide at the most intense isotope distribution was used as relative peak intensity. The mass spectrometric heterogeneity of the Fc-glycosylation sites of IgG1 (Fig. 7A) and IgG2 (Fig. 7B) was consistent with those of the commercially available polyclonal IgG (Fig. 5B and D) and previous reports [29]. The glycosylation pattern of haptoglobin at each site was similar to that of the commercially available haptoglobin except that peak intensities of minor glycoforms were noise level (Figs. 6B–E and 7D–F). The glycosylation of transferrin (Fig. 7G and H) at each site was consistent with previous reports [29]. Three glycopeptides of the four expected ones derived from ceruloplasmin could be assigned on the chromatogram of the serum sample (Fig. 7I–K), and their glycosylation patterns were in agreement with those in our previous reports [28]. Table 1 summarized LC retention time, *m/z* and charge, relative peak intensities of assigned glycopeptides in LC/MS. No O-glycosylated peptides were detected in this study. It would be due to low amount of O-glycosylation in serum and huge sample complexity.

4. Discussion

Alteration of glycans in several serum glycoproteins is a potential marker for several diseases. Several glycomic approaches to the diagnosis using mass spectrometric techniques have been proposed. The most common procedure involves analyzing the liberated glycans by MALDI-TOF MS or LC/ESI-MS, but this method provides no information on the glycosylation sites or protein sources. Another approach involves mass spectrometric analysis of glycopeptides resulting from proteolytic digestion. The enrichment of glycopeptides is useful due to their low ionization efficiency, but loss of glycopeptides cannot be avoidable. In the present study, we performed LC/MS(/MS) with high resolution separation to obtain